Springer

Journal of Mechanical Science and Technology

Journal of Mechanical Science and Technology 23 (2009) 1650~1669

www.springerlink.com/content/1738-494x
DOI 10.1007/s12206-009-0355-y

Two -fluid nonlinear mathematical model for pulsatile blood flow through catheterized arteries †

D. S. Sankar and Usik Lee*

Department of Mechanical Engineering, Inha University, 253 Yonghyun-Dong, Nam-Gu, Incheon 402-751, Republic of Korea
(Currently working at the School of Mathematical Sciences, University Science Malaysia, 11800 Penang, Malaysia)

(Manuscript Received February 25, 2008; Revised October 8, 2008; Accepted February 25, 2009)

Abstract

The pulsatile flow of blood through a catheterized artery is analyzed, assuming the blood as a two-fluid model with the suspension of all the erythrocytes in the core region as a Herschel-Bulkley fluid and the peripheral region of plasma as a Newtonian fluid. The resulting system of the nonlinear implicit system of partial differential equations is solved by perturbation method. The expressions for shear stress, velocity, flow rate, wall shear stress and longitudinal impedance are obtained. The variations of these flow quantities with yield stress, catheter radius ratio, amplitude, pulsatile Reynolds number ratio and peripheral layer thickness are discussed. The velocity and flow rate are observed to decrease, and the wall shear stress and resistance to flow increase when the yield stress increases. The plug flow velocity and flow rate decrease, and the longitudinal impedance increases when the catheter radius ratio increases. The velocity and flow rate increase while the wall shear stress and longitudinal impedance decrease with the increase of the peripheral layer thickness. The estimates of the increase in the longitudinal impedance are significantly lower for the present two-fluid model than those of the single-fluid model.

Keywords: Two-fluid model; Herschel-bulkley fluid; Newtonian fluid; Pulsatile flow; Catheterized artery; Longitudinal impedance

1. Introduction

Catheters are used extensively in modern medicine. Typically, a catheter consists of a long flexible cylindrical tube at the tip of which various functional tools (pressure transducers, flow meters, inflatable balloons, etc.) are positioned. The purpose of catheters is to accurately measure the arterial pressure or pressure gradient, or to clear short occlusions from the walls of the stenosed artery [1]. The method of catheterization is to insert the catheter-tool device into a peripheral artery and then position the device in the desired part of the arterial network by passing an appropriate length of the catheter through the artery [2]. The insertion of a catheter into an artery leads to the formation of an annular region between the catheter wall and the arterial wall. The insertion of a catheter into an artery alters the flow field, modifies the pressure distribution and hence increases the resistance to flow [3]. Thus, the pressure or pressure gradient recorded by a transducer attached to the catheter will differ from that of an uncatheterized artery and hence, it is essential to know the catheter-induced error [4].

Back [5] and Back et al. [6] have studied the important hemodynamic characteristics like the wall shear stress, pressure drop and frictional resistance in catheterized coronary arteries under the normal and pathological situation of a stenosis present. The effect of catheterization on various flow quantities in a curved artery is studied by Karahalios [7] and Jayaraman and Tiwari [8]. Daripa and Dash [1] have performed a numerical study of pulsatile blood flow in an eccentric catheterized artery using a fast algo-

† This paper was recommended for publication in revised form by Associate Editor Gihun Son

*Corresponding author. Tel.: +82 32 860 7318, Fax.: +82 32 866 1434
E-mail address: ulee@inha.ac.kr (U. Lee)

rithm. Apart from the above investigations, some more attempts [9-11] have been made to study the blood flow through catheterized arteries, treating blood as a Newtonian fluid. But, blood being a suspension of erythrocytes exhibits remarkable non-Newtonian behavior when it flows through narrow blood vessels at low shear rates [12, 13]. Since the blood flow through narrow arteries is highly pulsatile, many researchers [4, 14] have dealt with the pulsatile flow of blood flow through catheterized arteries by treating blood as a non-Newtonian fluid.

Bugliarello and Sevilla [15] and Cokelet [16] have shown through experiments that for blood flowing through narrow blood vessels, there is a peripheral layer of plasma which is a Newtonian fluid and a core region of suspension of all the erythrocytes which is non-Newtonian. Further, they have reported that it is impossible to represent the velocity distribution of blood flow through narrow arteries by a single-fluid model. For a realistic description of blood flow, it is appropriate to assume the blood as a two-fluid model with the suspension of all the erythrocytes in the core region as a non-Newtonian fluid and the plasma in the peripheral layer as a Newtonian fluid [17, 18]. Sankar and Lee [19] have reported that the two–fluid Herschel-Bulkley (H-B) model is more suitable to represent the blood when it flows through narrow blood vessels.

Sankar and Hemalatha [3] have analyzed the pulsatile flow of a single-fluid model for blood flow through catheterized artery, assuming blood as an H-B fluid. Sankar and Lee [20] have analyzed the steady flow of a two-fluid H-B model and estimated the increase in the resistance to flow due to catheterization. The pulsatile flow of the two-fluid model of blood through catheterized artery has not been studied so far by any one. Hence, in this model, we study the pulsatile flow of a two-fluid model for blood through catheterized narrow arteries (of diameters 0.02mm – 0.2mm) at low shear rates $(\dot{\gamma} < 10/\text{sec})$, assuming the suspension of all the erythrocytes in the core region of the blood vessel as an H-B fluid and the plasma in the peripheral layer as a Newtonian fluid. The layout of the paper is as follows.

Section 2 formulates the model mathematically, while section 3 nondimensionalizes the basic governing equations and the boundary conditions. The resulting implicit system of nonlinear equations is solved by perturbation method in section 4. The effects of pulsatility, catheterization, non-Newtonian nature of blood and peripheral layer thickness on various flow quantities are analyzed with some possible applications in section 5. The results are summarized, and some scope and possible extension of the present study are mentioned in the concluding section 6.

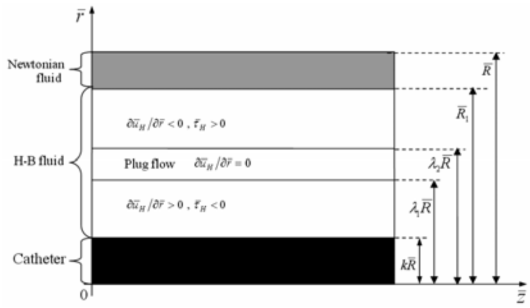

Fig. 1. Flow geometry of the catheterized artery.

2. Formulation of basic equations

Consider an axially symmetric, pulsatile, laminar, and fully developed flow of blood in an artery of radius $\bar{R}$ in which a catheter of radius $k\bar{R}\ (k<1)$ is introduced coaxially and blood is modeled as a two-fluid model with the suspension of all the erythrocytes in the core region as an H-B fluid and the plasma in the peripheral region as a Newtonian fluid. It is assumed that the pulsatile flow in the artery is due to a prescribed periodic pressure gradient along the axis of the artery. The length of the artery is assumed to be large enough when compared to its diameter so that entrance, end and special wall effects can be neglected. The cylindrical polar coordinate system $(\bar{r}, \bar{\phi}, \bar{z})$ is used to study the flow, where $\bar{r}$ and $\bar{z}$ denote the radial and axial coordinates and $\bar{\phi}$ is the azimuthal angle. The geometry of the catheterized artery is shown in Fig. 1. It can be shown that the radial velocity is negligibly small in magnitude and may be neglected for low Reynolds number flow. The basic momentum equations in this case simplify to

$$\bar{\rho}_H \frac{\partial \bar{u}_H}{\partial \bar{t}} = -\frac{\partial \bar{p}}{\partial \bar{z}} - \frac{1}{\bar{r}}\frac{\partial}{\partial \bar{r}}\left(\bar{r}\bar{\tau}_H\right) \quad \text{if} \quad k\bar{R} \le \bar{r} \le \bar{R}_1 \qquad (1)$$

$$\bar{\rho}_N \frac{\partial \bar{u}_N}{\partial \bar{t}} = -\frac{\partial \bar{p}}{\partial \bar{z}} - \frac{1}{\bar{r}}\frac{\partial}{\partial \bar{r}}\left(\bar{r}\bar{\tau}_N\right) \quad \text{if} \quad \bar{R}_1 \le \bar{r} \le \bar{R} \qquad (2)$$

where $\bar{p}$ denotes the pressure; $\bar{\rho}_H$ and $\bar{\rho}_N$ denote the density of the H-B fluid and Newtonian fluid, respectively; $\bar{\tau}_H$ and $\bar{\tau}_N$ denote the shear stress of the H-B fluid and Newtonian fluid, respectively; $\bar{u}_H$ and $\bar{u}_N$ denote the fluid's velocity in the core region and peripheral region, respectively; $\bar{t}$ denotes the time and $\bar{R}_1$ is the radius of the core region of the artery. We have assumed the Eqs. (3)-(5) of Sankar and Lee [20] as the constitutive equations of the fluids in motion in the core region (H-B fluid) and in the peripheral region (Newtonian fluid), and these equations are simplified to

$$\bar{\mu}_H \frac{\partial \bar{u}_H}{\partial \bar{r}} = \left|\bar{\tau}_H\right|^n \left(1 - \frac{n\bar{\tau}_y}{\left|\bar{\tau}_H\right|}\right) \quad \text{if} \quad \frac{\partial \bar{u}_H}{\partial \bar{r}} > 0, \quad \bar{\tau}_H < 0 \ \text{ and } \ k\bar{R} \le \bar{r} \le \lambda_1 \bar{R} \tag{3}$$

$$\bar{\mu}_H \frac{\partial \bar{u}_H}{\partial \bar{r}} = 0 \ \textit{if} \ \lambda_1 \bar{R} \le \bar{r} \le \lambda_2 \bar{R} \tag{4}$$

$$\bar{\mu}_H \frac{\partial \bar{u}_H}{\partial \bar{r}} = -\left|\bar{\tau}_H\right|^n \left(1 - \frac{n\bar{\tau}_y}{\left|\bar{\tau}_H\right|}\right) \quad \text{if} \quad \frac{\partial \bar{u}_H}{\partial \bar{r}} < 0, \quad \bar{\tau}_H > 0 \ \text{ and } \ \lambda_2 \bar{R} \le \bar{r} \le \bar{R}_1 \tag{5}$$

$$\bar{\mu}_N \frac{\partial \bar{u}_N}{\partial \bar{r}} = -\left|\bar{\tau}_N\right| \quad \text{if} \quad \frac{\partial \bar{u}_N}{\partial \bar{r}} < 0, \quad \bar{\tau}_N > 0 \ \text{ and } \ \bar{R}_1 \le \bar{r} \le \bar{R} \tag{6}$$

where $\bar{\mu}_H, \bar{\mu}_N$ are the viscosities of the H-B fluid and Newtonian fluid; $\bar{\tau}_y$ is the yield stress; λ_1 and λ_2 are the yield planes bounding the plug flow region. The details of the obtained Eqs. (3)-(6) are given in Sankar and Lee [20]. For the appropriate boundary conditions of the fluid flow, one can refer to Eqs. (11) and (12) of Sankar and Lee [20].

3. Nondimensionalization

Let $\bar{p}_0$ be the absolute magnitude of the typical pressure gradient. In addition Let us introduce the following nondimensional variables:

$$\begin{aligned} &u_H = \bar{u}_H \big/ \left(\bar{p}_0 \bar{R}^2 / 2\bar{\mu}_0\right), \\ &u_N = \bar{u}_N \big/ \left(\bar{p}_0 \bar{R}^2 / 2\bar{\mu}_N\right), \ r = \bar{r}/\bar{R}, \ R_1 = \bar{R}_1/\bar{R}, \\ &z = \bar{z}/\bar{R}, \ \tau_H = \bar{\tau}_H \big/ \left(\bar{p}_0 \bar{R}/2\right), \ \ \tau_N = \bar{\tau}_N \big/ \left(\bar{p}_0 \bar{R}/2\right), \\ &\theta = \bar{\tau}_y \big/ \left(\bar{p}_0 \bar{R}/2\right) \\ &t = \bar{\omega}\bar{t}, \ \varepsilon_H = \alpha_H^2 = \bar{R}_0^2 \bar{\rho}_H \bar{\omega}/\bar{\mu}_0, \\ &\varepsilon_N = \alpha_N^2 = \bar{R}_0^2 \bar{\rho}_N \bar{\omega}/\bar{\mu}_N \end{aligned} \tag{7}$$

where $\bar{\mu}_0 = \bar{\mu}_H \left(2/\bar{p}_0 \bar{R}\right)^{n-1}$ is the typical viscosity coefficient having the dimension as that of the Newtonian fluid's viscosity, α_H and α_N are the pulsatile Reynolds numbers of the H-B fluid and Newtonian fluid, respectively, and θ is the nondimensional yield stress. The pressure gradient can be written as

$$\frac{\partial \bar{p}}{\partial \bar{z}}\left(\bar{t}\right) = -\bar{p}_0 \, P(t) \tag{8}$$

where *P (t)* is the nondimensional pressure gradient along the axis, which is taken as a periodic function of time for pulsatile flow. Since the flow is pulsatile, the pressure gradient is taken as *P (t) = 1+ A sin t*, where A is the amplitude parameter. Using Eqs. (7) and (8), the momentum Eqs. (1) and (2) are simplified, respectively, to

$$\varepsilon_H \frac{\partial u_H}{\partial t} = 2P(t) - \frac{1}{r}\frac{\partial}{\partial r}\left(r\tau_H\right) \quad \text{if} \ \ k \le r \le R_1 \tag{9}$$

$$\varepsilon_N \frac{\partial u_N}{\partial t} = 2P(t) - \frac{1}{r}\frac{\partial}{\partial r}\left(r\tau_N\right) \quad \text{if} \ \ R_1 \le r \le 1 \tag{10}$$

Similarly, using Eqs. (7) and (8), the constitutive Eqs. (3)-(6) are simplified respectively to

$$\frac{\partial u_H}{\partial r} = \left|\tau_H\right|^n \left(1 - \frac{n\theta}{\left|\tau_H\right|}\right) \quad \text{if} \quad \frac{\partial u_H}{\partial r} > 0, \quad \tau_H < 0 \ \text{ and } \ k \le r \le \lambda_1 \tag{11}$$

$$\frac{\partial u_H}{\partial r} = 0 \quad \text{if} \quad \left|\tau_H\right| \le \theta \ \text{ and } \ \lambda_1 \le r \le \lambda_2 \tag{12}$$

$$\frac{\partial u_H}{\partial r} = -\left|\tau_H\right|^n \left(1 - \frac{n\theta}{\left|\tau_H\right|}\right) \quad \text{if} \quad \frac{\partial u_H}{\partial r} < 0, \quad \tau_H > 0 \ \text{ and } \ \lambda_2 \le r \le R_1 \tag{13}$$

$$\frac{\partial u_N}{\partial r} = -\left|\tau_N\right| \ \text{ if } \ \frac{\partial u_N}{\partial r} < 0, \ \tau_N > 0 \ \text{and} \ R_1 \le r \le 1 \tag{14}$$

One can refer to Eqs. (21) and (22) of Sankar and Lee [20] as the boundary conditions in the nondimensional form.

4. Perturbation method

As it is not possible to find an analytic solution of the nonlinear coupled implicit system of partial differential Eqs. (9)-(14), a perturbed method is used to solve the system of partial differential equations. When we nondimensionalize Eqs. (1) and (2), the pulsatile Reynolds numbers α_H and α_N occur naturally and hence it is appropriate to expand the unknowns τ_H, τ_N, u_H and u_N in powers of $\varepsilon_H = \alpha_H^2$ and $\varepsilon_N = \alpha_N^2$. The shear stress u_H of H-B fluid in the core region can be expanded in perturbation series as

$$u_H(r,t) = u_{0H}(r,t) + \varepsilon_H u_{1H}(r,t) + ... \quad (15)$$

Similarly one can expand τ_H, u_N and τ_N in the perturbation series as above. Substituting the perturbation expansions of u_H and τ_H in the momentum Eq. (9) and then equating the constant terms and ε_H terms (Since $\varepsilon_H << 1$, we have neglected the terms containing ε_H^2 and higher powers of ε_H), one can obtain

$$0 = 2P(t) - \frac{1}{r}\frac{\partial}{\partial r}(r\tau_{0H}) \quad (16)$$

$$\frac{\partial u_{0H}}{\partial t} = -\frac{1}{r}\frac{\partial}{\partial r}(r\tau_{1H}) \quad (17)$$

Hereafter, for convenience, we have used 'P' instead of 'P (t)'. Using the perturbation series expansions of u_N and τ_N in Eq. (10) and then equating the constant terms and ε_N terms, we get

$$0 = 2P - \frac{1}{r}\frac{\partial}{\partial r}(r\tau_{0N}) \quad (18)$$

$$\frac{\partial u_{0N}}{\partial t} = -\frac{1}{r}\frac{\partial}{\partial r}(r\tau_{1N}) \quad (19)$$

Using the perturbation series expansion of u_H and τ_H in Eqs. (11)-(13) and then equating the constant terms and ε_H terms, we obtain
when $k \le r \le \lambda$

$$\frac{\partial u_{0H}}{\partial r} = |\tau_{0H}|^{n-1}\left(|\tau_{0H}| - n\theta\right) \text{ if } \frac{\partial u_{0H}}{\partial r} > 0 \text{ and } \tau_{0H} < 0 \quad (20)$$

$$\frac{\partial u_{1H}}{\partial r} = n|\tau_{0H}|^{n-2}|\tau_{1H}|\left(|\tau_{0H}| - (n-1)\theta\right) \quad \text{if } \frac{\partial u_{1H}}{\partial r} > 0 \text{ and } \tau_{1H} < 0 \quad (21)$$

when $\lambda_1 \le r \le \lambda_2$

$$\frac{\partial u_{0H}}{\partial r} = 0 \qquad \text{if } |\tau_{0H}| < \theta \quad (22)$$

$$\frac{\partial u_{1H}}{\partial r} = 0 \qquad \text{if } |\tau_{1H}| < \theta \quad (23)$$

when $\lambda_2 \le r \le R_1$

$$\frac{\partial u_{0H}}{\partial r} = -|\tau_{0H}|^{n-1}\left(|\tau_{0H}| - n\theta\right) \text{ if } \frac{\partial u_{0H}}{\partial r} < 0 \text{ and } \tau_{0H} > 0 \quad (24)$$

$$\frac{\partial u_{1H}}{\partial r} = -n|\tau_{0H}|^{n-2}|\tau_{1H}|\left(|\tau_{0H}| - (n-1)\theta\right) \quad \text{if } \frac{\partial u_{1H}}{\partial r} < 0 \text{ and } \tau_{1H} > 0 \quad (25)$$

Using the perturbation series expansion of u_N and τ_N in Eq. (14) and then equating the constant terms and ε_N terms, one can get

$$\frac{\partial u_{0N}}{\partial r} = -\tau_{0N} \quad \text{if } \frac{\partial u_{0N}}{\partial r} < 0, \quad \tau_{0N} > 0 \text{ and } R_1 \le r \le 1 \quad (26)$$

$$\frac{\partial u_{1N}}{\partial r} = -\tau_{1N} \text{ if } \frac{\partial u_{1N}}{\partial r} < 0, \ \tau_{1N} > 0 \text{ and } R_1 \le r \le 1 \quad (27)$$

Using the perturbation series expansion of u_H, τ_H, u_N and τ_N, Eqs. (21) and (22) (the boundary conditions in the non-dimensional form) of Sankar and Lee [20] become

$$u_{0H} = u_{1H} = 0 \text{ at } r = k \text{ and } u_{0N} = u_{1N} = 0 \text{ at } r = 1 \quad (28)$$

$$u_{0H} = u_{0N};\ u_{1H} = u_{1N};\quad \tau_{oH} = \tau_{0N} \text{ and } \tau_{1H} = \tau_{1N} \quad r = R_1 \quad (29)$$

Note that the initial components $\tau_{0H}, \tau_{0N}, u_{0H}$ and u_{0N} of the flow quantities τ_H, τ_N, u_H and u_N are the same as the flow quantities τ_H, τ_N, u_H and u_N of the steady flow. Thus, solving Eqs. (20), (22), (24) and (26), the expressions for $\tau_{0H}, \tau_{0N}, u_{0H}$ and u_{0N} are obtained as

$$\tau_{0H} = (P/r)(r^2 - \lambda^2) \quad (30)$$

$$\tau_{0N} = (P/r)(r^2 - \lambda^2) \quad (31)$$

$$u_{0H}^{+} = P^n\left[\int_k^r \left(\frac{\lambda^2 - x^2}{x}\right)^n dx - n\beta\int_k^r \left(\frac{\lambda^2 - x^2}{x}\right)^{n-1} dx\right] \quad (32)$$

$$u_{0p} = P^n\left[\int_k^{\lambda_1} \left(\frac{\lambda^2 - x^2}{x}\right)^n dx - n\beta\int_k^{\lambda_1} \left(\frac{\lambda^2 - x^2}{x}\right)^{n-1} dx\right] \quad (33)$$

$$u_{oH}^{++} = P^n\left[\int_r^{R_1} \left(\frac{x^2 - \lambda^2}{x}\right)^n dx - n\beta\int_r^{R_1} \left(\frac{x^2 - \lambda^2}{x}\right)^{n-1} dx\right] \quad (34)$$

$$u_{0N} = \frac{P}{2}\left[1 - r^2 + 2\lambda^2 \log r\right] \quad (35)$$

where

$$\lambda^2 = \lambda_1 \lambda_2 \quad (36)$$

$$\lambda_2 - \lambda_1 = (\theta/P) = \beta \quad (37)$$

where β is the width of the plug core region. Note that u_{0H}^{+}, u_{op} and u_{0H}^{++} denote the initial approximation to the fluid's velocity in the regions $k \le r \le \lambda_1$, $\lambda_1 \le r \le \lambda_2$ and $\lambda_2 \le r \le R_1$, respectively. The details of obtaining Eq. (30)-(37) are given in Sankar and Lee [20], as these are the corresponding flow quantities of the steady flow. By the continuity of the velocity distribution throughout the flow field, we have the condition

$$u_{0H}^{+}(r=\lambda_1) = u_{0p} = u_{0H}^{++}(r=\lambda_2) \quad (38)$$

This gives

$$P^n \left\{ \int_k^{\lambda_1} \left(\frac{\lambda^2 - r^2}{r} \right)^n dr - \int_{\lambda_2}^{R_1} \left(\frac{r^2 - \lambda^2}{r} \right)^n dr - n\beta \left[\int_k^{\lambda_1} \left(\frac{\lambda^2 - r^2}{r} \right)^{n-1} dr - \int_{\lambda_2}^{R_1} \left(\frac{r^2 - \lambda^2}{r} \right)^{n-1} dr \right] \right\} - \frac{P}{2}\left[1 - R_1^2 + 2\lambda^2 \log(R_1) \right] = 0 \quad (39)$$

Using Eqs. (36) and (37) in Eq. (39), one can get

$$P^n \left\{ \int_k^{\lambda_1} \left(\frac{\lambda_1(\lambda_1+\beta) - r^2}{r} \right)^n dr - \int_{\lambda_1+\beta}^{R_1} \left(\frac{r^2 - \lambda_1(\lambda_1+\beta)}{r} \right)^n dr - n\beta \left[\int_k^{\lambda_1} \left(\frac{\lambda_1(\lambda_1+\beta) - r^2}{r} \right)^{n-1} dr - \int_{\lambda_1+\beta}^{R_1} \left(\frac{r^2 - \lambda_1(\lambda_1+\beta)}{r} \right)^{n-1} dr \right] \right\} - \frac{P}{2}\left[1 - R_1^2 + 2\lambda^2 \log(R_1) \right] = 0 \quad (40)$$

The above equation is solved numerically for λ_1 using Regula–Falsi method, the integrals are evaluated numerically using quadrature formula. Once λ_1 is known, λ_2 is determined using Eq. (38). Integration of Eq. (21) yields the correction to shear stress τ_H of the H-B fluid due to small inertial effects as

$$\tau_{1H} = \frac{1}{r} \int_r^{\lambda} \frac{\partial u_{0H}}{\partial t} r\, dr + \frac{D(t)}{r} \quad (41)$$

where $D(t) = \lambda \tau_{1H}(\lambda, t)$ is an unknown function of time which is to be determined. The details of derivation of τ_{1H} are given in Appendix 1. The corrected shear stress distribution of τ_H is $\tau_{0H} + \varepsilon_H \tau_{1H}$. Due to this corrected shear stress, the yield planes λ_1 and λ_2 will be shifted. Let the corrected yield plane locations be $\lambda_1 + \varepsilon_H \lambda_1^C$ and $\lambda_2 + \varepsilon_H \lambda_2^C$. Eq. (43) can be rewritten as

$$-\left(\tau_{0H} + \varepsilon_H \tau_{1H} \right)\Big|_{r=\lambda_1+\varepsilon_H\lambda_1^C} = \theta = \tau_{0H} + \varepsilon_H \tau_{1H}\Big|_{r=\lambda_2+\varepsilon_H\lambda_2^C} \quad (42)$$

Using Taylor series expansion and making use of Eq. (43), one can obtain

$$\lambda_1^C = \frac{-\tau_{1H}(\lambda_1, t)}{\frac{\partial \tau_{0H}}{\partial r}(\lambda_1, t)} \quad (43)$$

$$\lambda_2^C = \frac{-\tau_{1H}(\lambda_2, t)}{\frac{\partial \tau_{0H}}{\partial r}(\lambda_2, t)} \quad (44)$$

Integrating of Eq. (30) between R_1 and r and using the boundary condition $\tau_{1N}(R_1, t) = \tau_{1H}(R_1, t)$, one can obtain the correction to shear stress τ_N of the Newtonian fluid due to small inertial effects as

$$\tau_{1N} = -\frac{1}{r} \int_{R_1}^{r} \frac{\partial u_{0H}}{\partial t} r\, dr + \frac{R_1 \tau_{1N}(R_1, t)}{r} \quad (45)$$

The details of obtaining the final expression for τ_{1N} are given in Appendix 2. The details of obtaining the expressions for correction to velocity distribution u_{1H} and u_{1N} in the regions $k \le r \le \lambda_1$, $\lambda_1 \le r \le \lambda_2$, $\lambda_2 \le r \le R_1$ and $R_1 \le r \le 1$ are given in Appendix 3. The expression for $D(t)$ is also obtained in Appendix 3. The nondimensional flow rate is given by

$$Q = 8 \int_k^1 u\, r\, dr = 8 \left[\int_k^{\lambda_1} u_H^{+}\, r\, dr + \int_{\lambda_1}^{\lambda_2} u_p\, r\, dr + \int_{\lambda_2}^{R_1} u_H^{++}\, r\, dr + \int_{R_1}^{1} u_N\, r\, dr \right] \quad (46)$$

The expression for the flow rate Q is obtained in Appendix 4. The wall shear stress in the artery is obtained from Eqs. (31) and (A2.6) and is given by

$$\tau_w = \tau_N\big|_{r=1} = \tau_{0N}\big|_{r=1} + \varepsilon_N \tau_{1N}\big|_{r=1} = \tau_{0w} + \varepsilon_N \tau_{1w} \quad (47)$$

where

$$\tau_{0w} = P\left(1-\lambda^2\right) \tag{48}$$

and

$$\tau_{1w} = -\frac{1}{8}\frac{dP}{dt}\Big[2\left(1-R_1^2\right)-\left(1-R_1^4\right) + \lambda^2\left\{-4R_1^2\log R_1 - 2\left(1-R_1^2\right)\right\}\Big] + \frac{\lambda P}{2}\frac{d\lambda}{dt}\left[2R_1^2\log R_1 + 1 - R_1^4\right]$$
$$-nP^{n-1}\frac{dP}{dt}\left[\int_{y=\lambda_2}^{R_1}\int_{x=y}^{R_1}\left(\frac{x^2-\lambda^2}{x}\right)^n dx\, y\,dy - n\beta\int_{y=\lambda_2}^{R_1}\int_{x=y}^{R_1}\left(\frac{x^2-\lambda^2}{x}\right)^{n-1} dx\, y\,dy - \left(\frac{\lambda^2-\lambda_2^2}{2}\right)\left\{\int_k^{\lambda_1}\left(\frac{\lambda^2-x^2}{x}\right)^n dx - n\beta\int_k^{\lambda_1}\left(\frac{\lambda^2-x^2}{x}\right)^n dx\right\}\right]$$
$$+2n\lambda P^n\frac{d\lambda}{dt}\left[\int_{y=\lambda_2}^{R_1}\int_{x=y}^{R_1}\left(\frac{x^2-\lambda^2}{x}\right)^n \frac{dx}{\left(x^2-\lambda^2\right)}\,y\,dy - (n-1)\beta\int_{y=\lambda_2}^{R_1}\int_{x=y}^{R_1}\left(\frac{x^2-\lambda^2}{x}\right)^{n-1}\frac{dx}{\left(x^2-\lambda^2\right)}\,y\,dy + \left(\frac{\lambda^2-\lambda_2^2}{2}\right)\left\{\int_k^{\lambda_1}\left(\frac{\lambda^2-x^2}{x}\right)^n\frac{dx}{\left(\lambda^2-x^2\right)} - (n-1)\beta\int_k^{\lambda_1}\left(\frac{\lambda^2-x^2}{x}\right)^n\frac{dx}{\left(\lambda^2-x^2\right)}\right\}\right]$$
$$-\left(\frac{R_1^2-\lambda_2^2}{4}\right)\left(1-R_1^2+2\lambda^2\log R_1+4P\lambda\log R_1\right)+D(t) \tag{49}$$

The longitudinal impedance of the artery is given by

$$\Lambda = P/Q \tag{50}$$

when R_1 = 1.0, the present model reduces to the single-fluid H-B model for blood flow through catheterized arteries and is such a case, the expressions for shear stress, velocity, flow rate, wall shear stress and longitudinal resistance are in good agreement with those of Sankar and Hemalatha [20].

5. Numerical computation and discussion of results

The objective of the present study is to analyze the effects of the pulsatility, catheter, non–Newtonian nature of blood and peripheral layer thickness in a narrow artery, when a catheter is inserted into an artery coaxially. Blood has been modeled as a two-fluid model with the suspension of all the erythrocytes in the core region as an H–B fluid and the plasma in the peripheral layer as a Newtonian fluid. The single and multiple integrals appearing in the expressions of the flow quantities are evaluated numerically by using the quadrature formula. Similarly, the derivative dλ/dt occurring in the flow quantities is computed by numerical differentiation. Though the yield stress of blood at a haematocrit of 40 is $\bar{\tau}_y = 0.04\,dyne/cm^2$ [21], the range $\theta = 0$ to 0.1 is more suitable when a catheter is inserted into the blood vessels [4]. Just to pronounce the variations in the flow quantities (Velocity, flow rate, wall shear stress etc), we have taken the range of yield stress θ as 0 to 0.25 in this study. It is generally observed that the typical values of the power law index n for blood flow models are taken to lie between 0.9 and 1.1, and we have used the typical values of n to be 0.95 when $n < 1$ and 1.05 when $n > 1$ [14].

Since the flow is pulsatile and any periodic function can be represented by a Fourier series, it is appropriate to choose the pressure gradient as $P(t) = 1 + A\sin t$, where A is the amplitude parameter and is taken as less than 1. In the present study, we use the range 0.2-0.7 for the amplitude parameter A to discuss its influence [14]. The range of the catheter radius ratio k (ratio between the radius of the catheter and the radius of the artery) is taken as 0.1-0.7 to accommodate all the types of catheters. The fluid motion would be almost stopped if the range is increased further. When $k \to 0$, the present study reduces to the two-fluid blood flow model through a uniform tube. The values of the position of the interface R_1 between the core region and peripheral layer are taken as 0.95 and 0.985 [18, 19].

The ratio α (= α_N/α_H) between the pulsatile Reynolds numbers of the Newtonian fluid and H-B fluid is called the pulsatile Reynolds number ratio. Though the pulsatile Reynolds number ratio α ranges from 0 to 1, it is appropriate to assume its value as 0.5 [19]. Although the pulsatile Reynolds number α_H of the H-B fluid also ranges from 0 to 1 [14], the values 0.5 and 0.25 are used to analyze its effect on the flow quantities. Given the values of α and α_H, the value of α_N can be obtained from $\alpha = \alpha_N/\alpha_H$.

5.1 Yield plane locations

Since blood has a finite yield stress [13], it exhibits plug flow (solid-like flow) in regions where the shear

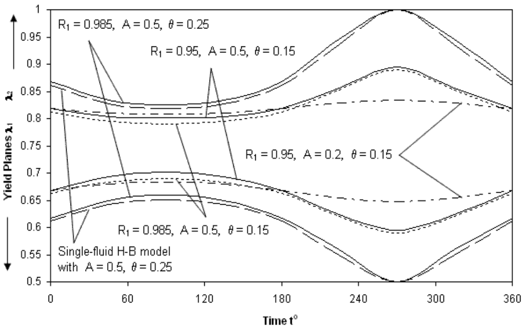

Fig. 2. Variation of yield plane locations in a time cycle for different values of R_1, A and θ with n = 0.95 and k = 0.5.

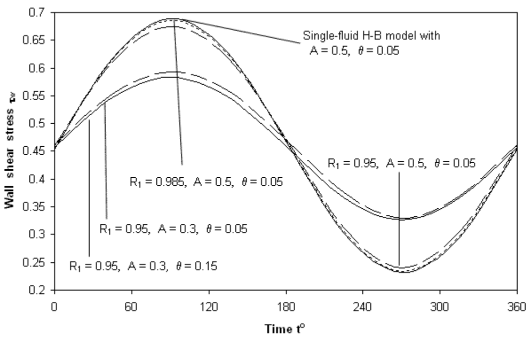

Fig. 3. Variation of wall shear stress in a time cycle for different values of R_1, A and θ with $k = \alpha_N$ = 0.5 and n = 0.95.

stress is less than the yield stress. The location of a point where the shear stress is equal to the yield stress is called a yield point and the locus of such points is called yield plane. For plain tube flow, there is only one yield plane, whereas in the case of annular tube flow, there exist two yield planes $r = \lambda_1$ and $r = \lambda_2$ which bound the plug flow region, and the difference $\lambda_1 - \lambda_2 = \beta$ is the width of the plug flow region. Since pulsatile flow is assumed, the yield planes λ_1, λ_2 and the width of the plug flow region β change with respect to time.

The variation of yield plane locations in a time cycle for different values of the interface position R_1, amplitude A and yield stress θ with n = 0.95 and k = 0.5 is depicted in Fig. 2. It is noted that the width of the plug flow region decreases as time t increases from 0° to 90°, then increases as t increases from 90° to 270° and then again it decreases as t increases further from 270° to 360°. The width of the plug flow region is minimum at 90° and maximum at 270°. For a given set of values of the parameters R_1 and A, the width of the plug flow region increases considerably with increasing values of the yield stress θ. For the

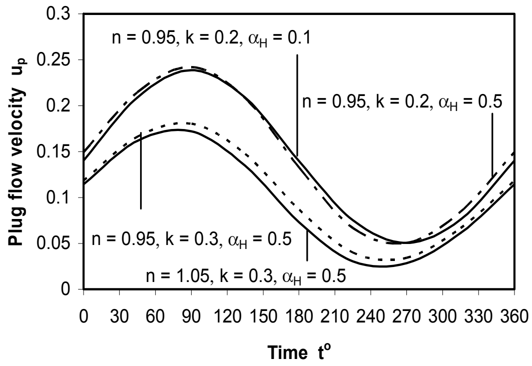

Fig. 4. Variation of plug flow velocity in a time cycle for different values of n, k and α_H with θ = 0.1, A = 0.5 and R_1 = 0.95.

fixed values of R_1 and θ and increasing values of the amplitude A, the width of the plug flow region decreases marginally when time t lies between 0° and 180° and increases significantly when t lies between 180° and 360°. But due to the variation of the interface position, there is no considerable change in the width of the plug flow region. From Fig. 2, the plot of the single-fluid H-B model is in good agreement with Fig. 2 of Sankar and Hemalatha [3]. Fig. 2 shows the effects of non-Newtonian nature of blood and the amplitude of the pulsatile flow of two-fluid model for blood through a catheterized artery.

5.2 Wall shear stress

Fig. 3 shows the variation of the wall shear stress for different values of the yield stress θ, amplitude A and the interface position R_1 with $k = \alpha_N$ = 0.5 and n = 0.95. It is noticed that the wall shear stress increases as time t increases from 0° to 90°, then decreases as t increases from 90° to 270°, and then again increases as t increases further from 270° to 360°. The wall shear stress is maximum at 90° and minimum at 270°. For the fixed values of the parameters A and R_1, the wall shear stress increases slightly as the yield stress θ increases, whereas the reverse behavior is observed when the thickness of the peripheral layer increases (R_1 decreases) while all the other parameters are held constant. For a given set of values of R_1 and θ and increasing values of the amplitude A, the wall shear stress increases significantly when time t lies between 0° and 180° and decreases considerably when t lies between 180° and 360°. The wall shear stress of the two-fluid H-B model is marginally lower than that of the single-fluid H-B model. It is worth mentioning that the plot of the single-fluid H-B model in Fig. 3 is in good agreement with Fig. 9 of Sankar and Hemalatha [3]. Fig. 3 depicts the effects of peripheral layer thickness and non-Newtonian nature of blood on wall shear stress in the two-fluid blood flow model.

5.3 Plug flow velocity

The variation of plug flow velocity in a time cycle for different values of the power law index n, catheter radius ratio k and pulsatile Reynolds number α_H of the H-B fluid with $\theta = 0.1$, $A = 0.5$ and $R_1 = 0.95$ is sketched in Fig. 4. The plug flow velocity increases as time t increases from 0° to 90°, then decreases as t increases from 90° to 270°, and then again increases from 270° to 360°. The plug flow velocity is maximum at 90° and minimum at 270°. For a given set of values of the pulsatile Reynolds number α_H and power law index *n* and the increasing values of catheter radius ratio *k*, the plug flow velocity decreases very significantly. Also, for a given set of values of the pulsatile Reynolds number α_H and the catheter radius ratio *k* and the increasing values of power law index *n*, the plug flow velocity decreases very slightly when the time parameter *t* lies between 0° and 90° and, 270° and 360° and, it decreases marginally when the time *t* lies between 90° and 270°. For a given set of values of *k* and *n* and increasing values of α_H, the plug flow velocity increases when time t lies between 0° and 90° and also between 270° and 360°, and it decreases when t lies between 90° and 270°. But the variation in the plug flow velocity due to the increase in the pulsatile Reynolds number α_H of the H-B fluid is marginal. Fig. 4 shows the effects of catheterization, pulsatility and non-Newtonian nature of the fluid on the plug flow velocity in the two-fluid model of blood flow.

5.4 Velocity distribution

Velocity distributions give a detailed description of the flow field. The velocity distributions during a time cycle with $A = 0.2$, $\alpha = \alpha_H = 0.5$, $\alpha_N = 0.25$, $k = 0.3$, $R_1 = 0.985$ and $\theta = 0.1$ for $n = 0.95$ and $n = 1.05$ are shown in Figs.5(a) and 5(b). One can notice the plug flow, around the middle of the velocity profile. The velocity increases from 0° to 90°, then decreases as t increases further from 90° to 270°, and then again increases from 270° to 360°. The velocity is maximum at 90° and minimum at 270°. At different instants of time t, the variations in the velocity profiles are highly significant around the plug flow region and

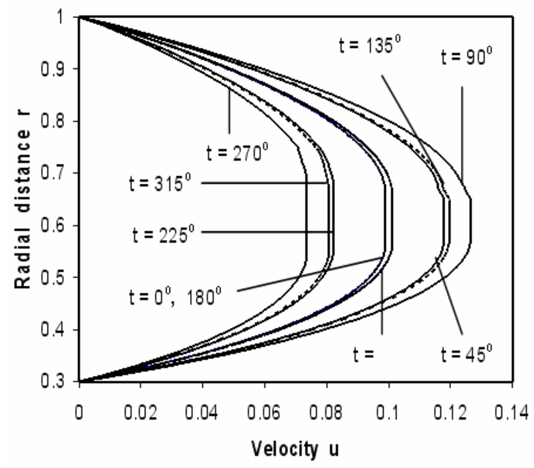

(a) $n = 0.95$

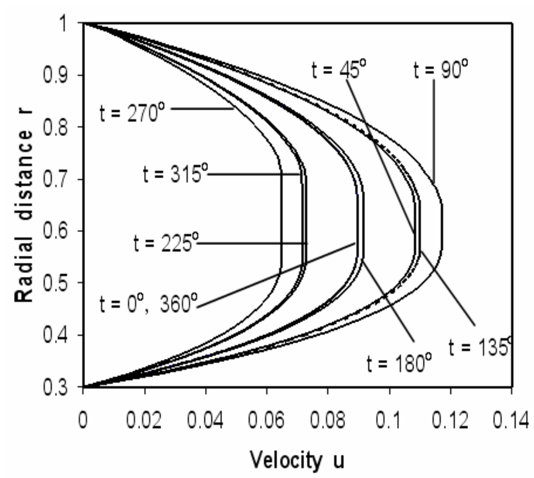

(b) $n = 1.05$

Fig. 5. Velocity distribution during a time cycle with $A = 0.2$, $\alpha = \alpha_H = 0.5$, $\alpha_N = 0.25$, $k = 0.3$, $R_1 = 0.985$ and $\theta = 0.1$.

these variations decrease rapidly in the radial direction and all the velocity profiles coincide at the walls of the blood vessel and the catheter. Furthermore, the velocity is marginally higher for $n = 0.95$ than that of $n = 1.05$. The velocity distribution for different values of A, R_1 and θ with $n = 0.95$, $\alpha = \alpha_H = 0.5$, $\alpha_N = 0.25$ and $k = 0.5$ is plotted in Fig. 6. For a given set of values of A and θ, the velocity increases considerably with the increase of the peripheral layer thickness (as R_1 decreases). The velocity increases significantly with the increase of the amplitude, whereas the behavior is reversed when the yield stress increases while the rest of the parameters kept fixed. One can notice that the plot of the single-fluid H-B model in

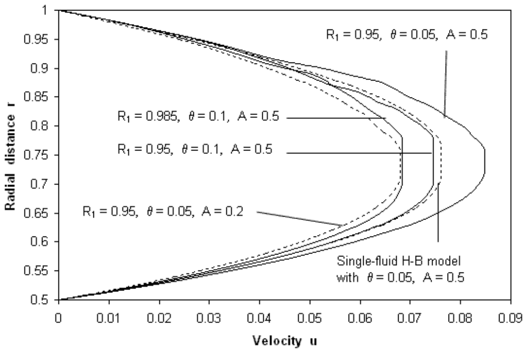

Fig. 6. Velocity distribution for different values of A, θ and R_1 with n = 0.95, $\alpha = \alpha_H = 0.5$, $\alpha_N = 0.25$ and k = 0.5.

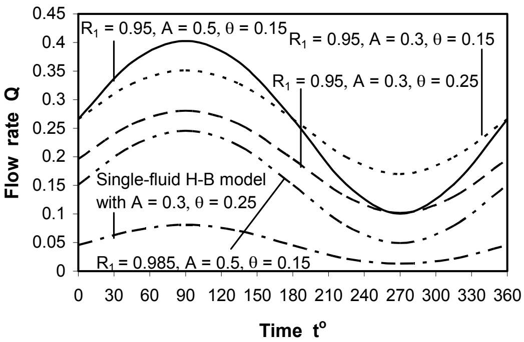

Fig. 7. Variation of flow rate in a time cycle for different values of R_1, A and θ with $\alpha_N = 0.25$, $k = \alpha = \alpha_H = 0.5$, and n = 0.95.

Fig. 6 is in good agreement with Fig. 5 of Sankar and Hemalatha [3]. Fig. 6 depicts the simultaneous effects of amplitude, peripheral layer thickness and non-Newtonian nature of the blood on the velocity distribution in the two-fluid blood flow model.

5.5 Flow rate

Fig. 7 shows the variation of the flow rate in a time cycle for different values of R_1, A and θ with $k = \alpha = \alpha_H = 0.5$, $\alpha_N = 0.25$ and $n = 0.95$. The flow rate increases as time t increases from 0° to 90°, then decreases as increases from 90° to 270°, and then again increases as t increases further from 270° to 360°. The increase in the flow rate is highly significant when the peripheral layer thickness R_1 increases and the flow rate increases considerably with the increase of the yield stress θ while all the other parameters are kept as invariable. For a given set of values of the parameters R_1 and θ and increasing values of the amplitude, the flow rate increases when the time t lies between 0° and 180° and decreases when t lies between 180° and 360°. It is of interest to note that the plot of the single-fluid H-B model is in good agreement with Fig. 7 of Sankar and Hemalatha [3]. Also, it is important to note that the flow rate of the two-fluid H-B model is considerably high compared with that of the single-fluid H-B model. The variation of flow rate in a time cycle for different values of the catheter radius ratio k and the power law index n with $R_1 = 0.95$, $A = \alpha = \alpha_H = 0.5$, $\alpha_N = 0.25$ and θ = 0.1 is plotted in Fig. 8. Clearly, the flow rate decreases significantly with the increase of the catheter radius ratio k when the power law index n is fixed. The same behavior is noticed when the power law index n increases, but the variation in the flow rate is very slight.

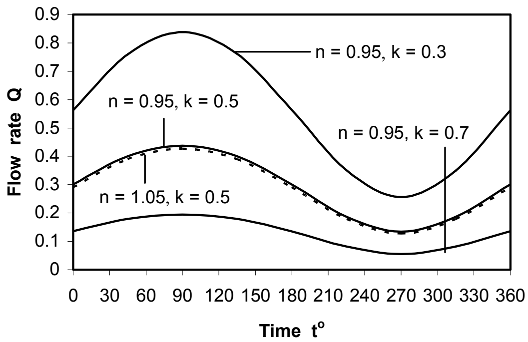

Fig. 8. Variation of flow rate in a time cycle for different values of n and k with $R_1 = 0.95$, $A = \alpha = \alpha_H = 0.5$, and θ = 0.1.

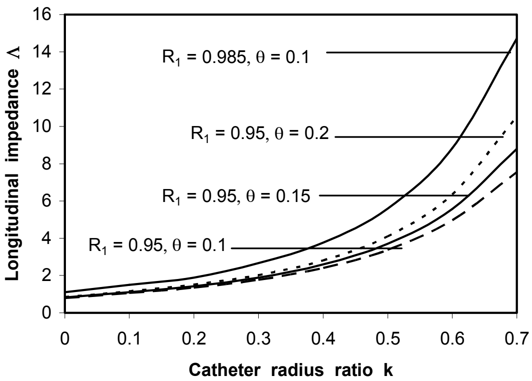

Fig. 9. Variation of longitudinal impedance with catheter radius ratio for different values of R_1 and θ with $A = \alpha = \alpha_H = 0.5$, n = 0.95 and t = 45°.

5.6 Longitudinal impedance

The variation of the longitudinal impedance with the catheter radius ratio for different values of R_1 and θ with $A = \alpha = \alpha_H = 0.5$, $\alpha_N = 0.25$, $n = 0.95$ and t =

45° is sketched in Fig. 9. The longitudinal impedance increases very slightly with the increase of the catheter radius ratio from 0 to 0.3, and it increases very rapidly (nonlinearly) when the catheter radius ratio increase further from 0.3 to 0.7. Also, for a given value of R_1, the impedance increases considerably with the increase of the yield stress, whereas the behavior is reversed when the peripheral layer thickness increases (R_1 decreases) while the yield stress θ is held constant. Fig. 9 shows the simultaneous effects of catheterization, non-Newtonian nature of the fluid and the peripheral layer thickness on longitudinal impedance of the two-fluid model of blood flow.

The increase in the longitudinal impedance due to the catheterization is defined as the ratio between the longitudinal impedance of a fluid model in a catheterized artery for a given set of values of the parameters and the longitudinal impedance of the same fluid in the uncatheterized artery for the same set of values of the parameters. This ratio specifically quantifies the effects of catheterization in the fluid flow. The estimates of the increase in the longitudinal impedance of the two-fluid and single-fluid H-B models for different values of the catheter radius ratio k and yield stress θ are computed in Table 1. For the range 0.1-0.7 of the catheter radius ratio, the ranges of increase in the estimates of the longitudinal impedance for the two-fluid H-B model and single-fluid H-B model are 1.34-9.51 and 1.4-33.49, respectively, when the yield stress is 0.1; 1.35-10.75 and 1.42-42.14, respectively, when the yield stress is 0.15 and, 1.37-12.46 and 1.44-56.57, respectively, when the yield stress is 0.2. It is clear that there is a substantial decrease in the estimates of the increase in the longitudinal impedance for the present two-fluid H-B model compared with those of the single-fluid H-B model. Also, the difference between the estimates of the two models is very significant when the catheter radius ratio k increases from 0.5 to 0.7. As a possible application of the present study to the medical field, the different types of catheters in clinical use, their range of size (Back, 1994) and the corresponding range of increase in the estimates of the longitudinal impedance for the two-fluid and single-fluid H-B models with n = 0.95 and n = 1.05 are presented in Table 2, where d_i and d_0 denote the diameter of the catheterized and uncatheterized arteries, respectively. It is of interest to observe that the range of the increase in the estimates of the longitudinal impedance for the present two-fluid H-B model is considerably lower than those of the single-fluid H-B model.

Table 1. The estimates of the increase in longitudinal impedance with catheter radius ratio k for different values of the yield stress θ for two-fluid and single-fluid models with effects on catheterization with $A = \alpha = \alpha_H = 0.5$, $\alpha_N = 0.25$, $n = R_1 = 0.95$ and $t = 45°$.

K	Two-fluid model			Single-fluid model		
	θ = 0.1	θ = 0.15	θ = 0.2	θ = 0.1	θ = 0.15	θ = 0.2
0.1	1.3356	1.3530	1.3719	1.4020	1.4224	1.4452
0.2	1.7141	1.7514	1.7933	1.8367	1.9593	2.0159
0.3	2.2427	2.3149	2.3972	2.7147	2.8241	2.9520
0.4	3.0298	3.1685	3.3297	4.1304	4.3798	4.6817
0.5	4.2573	4.5291	4.8573	6.9285	7.5569	8.3682
0.6	6.2416	6.8047	7.5181	13.4638	15.4046	18.1191
0.7	9.5072	10.7497	12.4575	33.4934	42.1378	56.5704

Table 2. Range of increase in longitudinal impedance for different types of catheters for two-fluid and single-fluid models with $A = \alpha = \alpha_H = 0.5$, $\alpha_N = 0.25$, $R_1 = 0.95$, t = 45° and θ = 0.1.

Type of catheter	Range of catheter size d_i/d_0	Two-fluid model		Single-fluid model	
		n = 0.95	n = 1.05	n = 0.95	n = 1.05
Guidewire	0.08 – 0.18	1.14 – 1.30	1.15 – 1.32	1.17 – 1.36	1.18 – 1.39
Infusion	0.14 – 0.33	1.24 – 1.57	1.25 – 1.60	1.28 – 1.71	1.31 – 1.77
Angioplasty catheter	0.3 – 0.7	1.51 – 2.31	1.54 – 2.39	1.63 – 3.05	1.68 – 2.30

6. Conclusions

Pulsatile flow of blood through catheterized arteries is analyzed in this paper, treating blood as a two-fluid model with the suspension of all the erythrocytes in the core region as an H-B fluid and the plasma in the peripheral layer as a Newtonian fluid. The velocity distribution and flow rate decrease, and, the wall shear, width of the plug flow region and longitudinal impedance decrease when the yield stress increases. Also, the velocity and flow rate increase, and the wall shear stress and the longitudinal impedance decrease when the thickness of the peripheral layer increases. The plug flow velocity and flow rate decrease, and the longitudinal impedance increases when the catheter radius ratio increases. Further, it is recorded that the increase in the estimates of the longitudinal impedance due to catheterization for the present two-fluid H-B model is considerably lower than those of the single-fluid H-B model. Hence, it is believed that the present two-fluid model could be considered as an improvement in the studies of blood flow. By using the present model, physicians can be more accurate in predicting the post-catheterization flow quantities. This study could be extended further by introducing the permeability of the wall of the artery and this would be done in the near future.

Aknowledgement

This work was supported by Inha University Research Grant.

References

[1] P. Daripa and R. K. Dash, A numerical study of pulsatile blood flow in an eccentric catheterized artery using a fast algorithms, *Journal of Engineering Mathematics,* 42 (2002) 1-22.

[2] M. A. MacDonald, Pulsatile flow in a catheterized artery, *Journal of Biomechanics,* 19 (1986) 239-249.

[3] D. S. Sankar and K. Hemalatha, Pulsatile flow of Herschel-Bulkley fluid for blood flow through a catheterized artery - A mathematical model, *Applied Mathematical Modeling,* 31 (2007) 1497-1517.

[4] R. K. Dash, G. Jayaraman and K. N. Metha, Estimation of increased flow resistance in a narrow catheterized artery – A theoretical model, *Journal of Biomechanics,* 29 (1996) 917-930.

[5] L. H. Back, Estimated mean flow resistance increase during coronary artery catheterization, *Journal of Biomechanics,* 27 (1994) 169-175.

[6] L. H. Back, E. Y. Kwack and M. R. Back, Flow rate-pressure drop relation in coronary angioplasty: catheter obstruction effect," *Journal of Biomechanical Engineering (ASME Trans),* 118 (1996) 83-89.

[7] G. T. Karahalios, Some Possible effects of a catheter on the arterial wall, *Medical Physics,* 17 (1990) 922-925.

[8] G. Jayaraman and K. Tiwari, Flow in a catheterized curved artery, *Medical and Biological Engineering and Computation,* 33 (1995) 1-6.

[9] R. K. Dash, G. Jayaraman and K. N. Metha, Flow in a catheterized artery with stenosis, *Journal of Biomechanics,* 32 (1999) 49-61.

[10] G. Jayaraman and R. K. Dash, Numerical study of flow in a constricted curved annulus: An application to flow in a catheterized artery, *Journal of Engineering Mathematics,* 40 (2001) 355-376.

[11] A. Sarkar and G. Jayaraman, Correction to flow rate–pressure drop relation in coronary angioplasty: steady streaming effect, *Journal Biomechanics,* 31 (1998), 781-791.

[12] P. Chaturani and R. Ponnalagar Samy, Pulsatile flow of a Casson fluid through stenosed arteries with application to blood flow, *Biorheology*, 23 (1986) 499-511.

[13] C. Tu and M. Deville, Pulsatile flow of non-Newtonian fluids through arterial stenosis, *Journal of Biomechanics,* 29 (1996) 899-908.

[14] D. S. Sankar and K. Hemalatha, Pulsatile flow of Herschel-Bulkley fluid through stenosed arteries - A mathematical model," *International Journal of Non-Linear Mechanics,* 41 (2006) 979-990.

[15] G. Bugliarello and J. Sevilla, Velocity distribution and other characteristics of steady and pulsatile blood flow in fine glass tubes, *Biorheology,* 7 (1970) 85-107.

[16] G. R. Cokelet, The rheology of human blood, In: Biomech. (Edited by Y.C. Fung), Prentice-Hall, N. J., U. S. A, 1972.

[17] J. C. Misra and S. K. Pandey, Peristaltic transport of blood in small vessels: Study of a mathematical model, *Computers and Mathematics with Applications,* 43 (2002) 1183-1193.

[18] V. P. Srivastava and M. Saxena, Two-layered model of Casson fluid flow through stenotic blood vessels: Applications to the cardiovascular system," *Journal Biomechanics,* 27 (1994) 921-928.

[19] D. S. Sankar and U. Lee, Two–phase non-linear model for the flow through stenosed blood vessels, *Journal of Mechanical Science and Technology,* 21 (2007) 678-689.

[20] D. S. Sankar and U. Lee, Two-fluid Herschel–Bulkley model for blood flow in catheterized arteries, *Journal of Mechanical Science and Technology*, 22 (2008) 1008-1018.

[21] E. W. Merrill, Rheology of blood, *Physiological Reviews,* 49 (1969) 863-888.

Appendix 1

We have as given in Eq. (42)

$$\tau_{1H} = \frac{1}{r}\int_{r}^{\lambda} \frac{\partial u_{0H}}{\partial r} r\, dr + \frac{D(t)}{r} \tag{A1.1}$$

As u_{0H} depends on t through P and λ, we shall write

$$\frac{\partial u_{0H}}{\partial t} = \frac{\partial u_{0H}}{\partial P}\frac{dP}{dt} + \frac{\partial u_{0H}}{\partial \lambda}\frac{d\lambda}{dt} \tag{A1.2}$$

Use of Eq. (A1.2) in Eq. (A1.1) gives

$$\tau_{1H} = \frac{1}{r}\left(\frac{dP}{dt}\int_r^{\lambda}\frac{\partial u_{0H}}{\partial P} r dr + \frac{d\lambda}{dt}\int_r^{\lambda}\frac{\partial u_{0H}}{\partial \lambda} r dr\right) + \frac{D(t)}{r} \tag{A1.3}$$

Hence, we have

$$\tau_{1H} = \frac{1}{r}\left(\frac{dP}{dt}\int_r^{\lambda_1}\frac{\partial u_{0H}^{+}}{\partial P} r\, dr + \frac{d\lambda}{dt}\int_r^{\lambda_1}\frac{\partial u_{0H}^{+}}{\partial \lambda} r\, dr\right) + \left(\frac{\lambda^2-\lambda_1^2}{2r}\right)\left(\frac{\partial u_{0P}}{\partial P}\frac{dP}{dt} + \frac{\partial u_{0P}}{\partial \lambda}\frac{d\lambda}{dt}\right) + \frac{D(t)}{r}$$

if $k \le r \le \lambda_1$ (A1.4)

$$\tau_{1p} = \left(\frac{\lambda^2-r^2}{2r}\right)\left(\frac{\partial u_{0P}}{\partial P}\frac{dP}{dt} + \frac{\partial u_{0P}}{\partial \lambda}\frac{d\lambda}{dt}\right) + \frac{D(t)}{r}$$

if $\lambda_1 \le r \le \lambda_2$ (A1.5)

$$\tau_{1H} = \left(\frac{\lambda^2-\lambda_2^2}{2r}\right)\left(\frac{\partial u_{0P}}{\partial P}\frac{dP}{dt} + \frac{\partial u_{0P}}{\partial \lambda}\frac{d\lambda}{dt}\right) - \frac{1}{r}\left(\frac{dP}{dt}\int_{\lambda_2}^{R_1}\frac{\partial u_{0H}^{++}}{\partial P} r\, dr + \frac{d\lambda}{dt}\int_{\lambda_2}^{R_1}\frac{\partial u_{0H}^{++}}{\partial \lambda} r\, dr\right) + \frac{D(t)}{r}$$

if $\lambda_2 \le r \le R_1$ (A1.6)

From Eqs. (50)-(52), we get

$$\frac{\partial u_{0H}^{+}}{\partial P} = nP^{n-1}\left[\int_k^r\left(\frac{\lambda^2-x^2}{x}\right)^n dx - n\beta\int_k^r\left(\frac{\lambda^2-x^2}{x}\right)^{n-1} dx\right]$$

if $k \le r \le \lambda_1$ (A1.7)

$$\frac{\partial u_{0p}}{\partial P} = nP^{n-1}\left[\int_k^{\lambda_1}\left(\frac{\lambda^2-x^2}{x}\right)^n dx - n\beta\int_k^{\lambda_1}\left(\frac{\lambda^2-x^2}{x}\right)^{n-1} dx\right]$$

if $\lambda_1 \le r \le \lambda_2$ (A1.8)

$$\frac{\partial u_{0H}^{++}}{\partial P} = nP^{n-1}\left[\int_r^{R_1}\left(\frac{x^2-\lambda^2}{x}\right)^n dx - n\beta\int_r^{R_1}\left(\frac{x^2-\lambda^2}{x}\right)^{n-1} dx\right] + \frac{1}{2}\left(1-R_1^2+2\lambda^2\log R_1\right)$$

if $\lambda_2 \le r \le R_1$ (A1.9)

$$\frac{\partial u_{0H}^{+}}{\partial \lambda} = 2n\lambda P^n\left[\int_k^r\left(\frac{\lambda^2-x^2}{x}\right)^n \frac{dx}{\left(\lambda^2-x^2\right)} - (n-1)\beta\int_k^r\left(\frac{\lambda^2-x^2}{x}\right)^{n-1}\frac{dx}{\left(\lambda^2-x^2\right)}\right]$$

if $k \le r \le \lambda_1$ (A1.10)

$$\frac{\partial u_{0p}}{\partial \lambda} = 2n\lambda P^n\left[\int_k^{\lambda_1}\left(\frac{\lambda^2-x^2}{x}\right)^n \frac{dx}{\left(\lambda^2-x^2\right)} - (n-1)\beta\int_k^{\lambda_1}\left(\frac{\lambda^2-x^2}{x}\right)^{n-1}\frac{dx}{\left(\lambda^2-x^2\right)}\right]$$

if $\lambda_1 \le r \le \lambda_2$ (A1.11)

$$\frac{\partial u_{0H}^{++}}{\partial \lambda} = -2n\lambda P^n\left[\int_r^{R_1}\left(\frac{x^2-\lambda^2}{x}\right)^n \frac{dx}{\left(x^2-\lambda^2\right)} - (n-1)\beta\int_r^{R_1}\left(\frac{x^2-\lambda^2}{x}\right)^{n-1}\frac{dx}{\left(x^2-\lambda^2\right)}\right] + 2P\lambda\log R_1$$

if $\lambda_2 \le r \le R_1$ (A1.12)

Substitution of Eqs. (A1.7)-(A1.12) in Eqs. (A1.4)-(A1.6) yields the shear stress as

$$\begin{aligned}\tau_{1H} = {} & \frac{nP^{n-1}}{r}\frac{dP}{dt}\left\{\int_{y=r}^{\lambda_1}\int_{x=k}^{y}\left(\frac{\lambda^2-x^2}{x}\right)^n dx \quad y\,dy - n\beta\int_{y=r}^{\lambda_1}\int_{x=k}^{y}\left(\frac{\lambda^2-x^2}{x}\right)^{n-1} dx \quad ydy\right\} \\ & + \left(\frac{\lambda^2-\lambda_1^2}{2}\right)\left[\int_k^{\lambda_1}\left(\frac{\lambda^2-x^2}{x}\right)^n dx - n\beta\int_k^{\lambda_1}\left(\frac{\lambda^2-x^2}{x}\right)^{n-1} dx\right]\Bigg\} \\ & + \frac{2n\lambda P^n}{r}\frac{d\lambda}{dt}\left\{\int_{y=r}^{\lambda_1}\int_{x=k}^{y}\left(\frac{\lambda^2-x^2}{x}\right)^n \frac{dx}{\left(\lambda^2-x^2\right)} \quad ydy - (n-1)\beta\int_{y=r}^{\lambda_1}\int_{x=k}^{y}\left(\frac{\lambda^2-x^2}{x}\right)^{n-1}\frac{dx}{\left(\lambda^2-x^2\right)} \quad ydy\right\} \\ & + \left(\frac{\lambda^2-\lambda_1^2}{2}\right)\left[\int_k^{\lambda_1}\left(\frac{\lambda^2-x^2}{x}\right)^n \frac{dx}{\left(\lambda^2-x^2\right)} - (n-1)\beta\int_k^{\lambda_1}\left(\frac{\lambda^2-x^2}{x}\right)^{n-1}\frac{dx}{\left(\lambda^2-x^2\right)}\right] + \frac{D(t)}{r}\end{aligned}$$

if $k \le r \le \lambda_1$ (A1.13)

$$\tau_{1p} = nP^{n-1}\left(\frac{\lambda^2-r^2}{2r}\right)\frac{dP}{dt}\left[\int_k^{\lambda_1}\left(\frac{\lambda^2-x^2}{x}\right)^n dx - n\beta\int_k^{\lambda_1}\left(\frac{\lambda^2-x^2}{x}\right)^{n-1} dx\right]$$

$$+2n\lambda P^n\left(\frac{\lambda^2-r^2}{2}\right)\frac{d\lambda}{dt}\left[\int_k^{\lambda_1}\left(\frac{\lambda^2-x^2}{x}\right)^n\frac{dx}{\left(\lambda^2-x^2\right)}\right.$$
$$\left.-(n-1)\beta\int_k^{\lambda_1}\left(\frac{\lambda^2-x^2}{x}\right)^{n-1}\frac{dx}{\left(\lambda^2-x^2\right)}\right]+\frac{D(t)}{r}$$

if $\lambda_1\le r\le\lambda_2$ (A1.14)

$$\tau_{1H}=-\frac{nP^{n-1}}{r}\frac{dP}{dt}$$
$$\left\{\left[\int_{y=\lambda_2}^{r}\int_{x=y}^{R_1}\left(\frac{x^2-\lambda^2}{x}\right)^n dx\,y\,dy-n\beta\int_{y=\lambda_2}^{r}\int_{x=y}^{R_1}\left(\frac{x^2-\lambda^2}{x}\right)^{n-1}dx\,y\,dy\right]\right.$$
$$\left.-\left(\frac{\lambda^2-\lambda_2^2}{2}\right)\left[\int_k^{\lambda_1}\left(\frac{\lambda^2-x^2}{x}\right)^n dx-n\beta\int_k^{\lambda_1}\left(\frac{\lambda^2-x^2}{x}\right)^{n-1}dx\right]\right\}$$
$$+\frac{2n\lambda P^n}{r}\frac{d\lambda}{dt}\left\{\left[\int_{y=\lambda_2}^{r}\int_{x=y}^{R_1}\left(\frac{x^2-\lambda^2}{x}\right)^n\frac{dx}{\left(x^2-\lambda^2\right)}y\,dy-(n-1)\beta\right.\right.$$
$$\left.\int_{y=\lambda_2}^{r}\int_{x=y}^{R_1}\left(\frac{x^2-\lambda^2}{x}\right)^{n-1}\frac{dx}{\left(x^2-\lambda^2\right)}y\,dy\right]$$
$$+\left(\frac{\lambda^2-\lambda_2^2}{2}\right)\left[\int_k^{\lambda_1}\left(\frac{\lambda^2-x^2}{x}\right)^n\frac{dx}{\left(\lambda^2-x^2\right)}-(n-1)\beta\right.$$
$$\left.\left.\int_k^{\lambda_1}\left(\frac{\lambda^2-x^2}{x}\right)^{n-1}\frac{dx}{\left(\lambda^2-x^2\right)}\right]\right\}$$
$$-\left(\frac{r^2-\lambda_2^2}{4r}\right)\left[1-R_1^2+2\lambda^2\log R_1+4P\lambda\log R_1\right]+\frac{D(t)}{r}$$

if $\lambda_2\le r\le R_1$ (A1.15)

Appendix 2

We have as given in Eq. (46)

$$\tau_{1N}=-\frac{1}{r}\int_{R_1}^{r}\frac{\partial u_{0N}}{\partial r}r\,dr+\frac{R_1\tau_{1H}\left(R_1,t\right)}{r} \tag{A2.1}$$

By the dependence of u_{0N} on t through P and λ, we have

$$\frac{\partial u_{0N}}{\partial t}=\frac{\partial u_{0N}}{\partial P}\frac{dP}{dt}+\frac{\partial u_{0N}}{\partial\lambda}\frac{d\lambda}{dt} \tag{A2.2}$$

Sustitution of Eq. (A2.2) in Eq. (A2.1) yields

$$\tau_{1N}=-\frac{1}{r}\left(\frac{dP}{dt}\int_{R_1}^{r}\frac{\partial u_{0N}}{\partial P}rdr+\frac{d\lambda}{dt}\int_{R_1}^{r}\frac{\partial u_{0N}}{\partial\lambda}rdr\right)+\frac{R_1\tau_{1H}\left(R_1,t\right)}{r} \tag{A2.3}$$

From Eq. (49), we have

$$\frac{\partial u_{0N}}{\partial P}=\frac{1}{2}\left(1-r^2+2\lambda^2\log r\right) \tag{A2.4}$$
$$\frac{\partial u_{0N}}{\partial\lambda}=2\lambda P\log r \tag{A2.5}$$

Substituting Eqs. (A2.4) and (A2.5) in Eq. (A2.3) and then integrating and using Eq. (A1.15), we obtain

$$\tau_{1N}=-\frac{1}{8r}\frac{dP}{dt}\left\{2\left(r^2-R_1^2\right)-\left(r^4-R_1^4\right)\right.$$
$$\left.+\lambda^2\left[4\left(r^2\log r-R_1^2\log R_1\right)-2\left(r^2-R_1^2\right)\right]\right\}$$
$$-\frac{\lambda P}{2r}\frac{d\lambda}{dt}\left[2\left(r^2\log r-R_1^2\log R_1\right)-\left(r^4-R_1^4\right)\right]$$
$$-\frac{nP^{n-1}}{r}\frac{dP}{dt}\left\{\int_{y=\lambda_2}^{R_1}\int_{x=y}^{R_1}\left(\frac{x^2-\lambda^2}{x}\right)^n dx\,y\,dy-n\beta\right.$$
$$\int_{y=\lambda_2}^{R_1}\int_{x=y}^{R_1}\left(\frac{x^2-\lambda^2}{x}\right)^{n-1}dx\,y\,dy$$
$$\left.-\left(\frac{\lambda^2-\lambda_2^2}{2}\right)\left[\int_k^{\lambda_1}\left(\frac{\lambda^2-x^2}{x}\right)^n dx-n\beta\int_k^{\lambda_1}\left(\frac{\lambda^2-x^2}{x}\right)^{n-1}\right]\right\}$$
$$+\frac{2n\lambda P^n}{r}\frac{d\lambda}{dt}\left\{\int_{y=\lambda_2}^{R_1}\int_{x=y}^{R_1}\left(\frac{x^2-\lambda^2}{x}\right)^n\frac{dx}{\left(x^2-\lambda^2\right)}y\,dy-(n-1)\beta\right.$$
$$\int_{y=\lambda_2}^{R_1}\int_{x=y}^{R_1}\left(\frac{x^2-\lambda^2}{x}\right)^{n-1}\frac{dx}{\left(x^2-\lambda^2\right)}y\,dy$$
$$+\left(\frac{\lambda^2-\lambda_2^2}{2}\right)\left[\int_k^{\lambda_1}\left(\frac{\lambda^2-x^2}{x}\right)^n\frac{dx}{\left(\lambda^2-x^2\right)}-(n-1)\beta\right.$$
$$\left.\left.\int_k^{\lambda_1}\left(\frac{\lambda^2-x^2}{x}\right)^{n-1}\frac{dx}{\left(\lambda^2-x^2\right)}\right]\right\}$$
$$-\left(\frac{R_1^2-\lambda_2^2}{4r}\right)\left(1-R_1^2+2\lambda^2\log R_1+4P\lambda\log R_1\right)+\frac{D(t)}{r}$$

if $R_1\le r\le 1$ (A2.6)

Appendix 3

Substituting Eqs. (A2.6) in Eq. (38) and then integrating the resulting equation between r and 1 with the help of the boundary condition (39) and simplifying, we get the correction to velocity distribution u_{1N} in the region $R_1\le r\le 1$ as

$$u_{1N}=-\frac{1}{8}\frac{dP}{dt}\left\{\left(1-r^2\right)+2R_1^2\log r-\frac{1}{3}\left(1-r^3\right)-R_1^4\log r\right.$$
$$\left.+\lambda^2\left[-2r^2\log r-2\left(1-r^2\right)+4R_1^2\log R_1\log r-2R_1^2\log r\right]\right\}$$

$$-\frac{\lambda P}{2}\frac{d\lambda}{dt}\left[-r^2\log r-\frac{1}{2}\left(1-r^2\right)\right.$$
$$\left.+2R_1^2\log R_1\log r-\frac{1}{3}\left(1-r^3\right)-R_1^4\log r\right]$$
$$+nP^{n-1}\log r\frac{dP}{dt}\left\{\int_{y=\lambda_2}^{R_1}\int_{x=y}^{R_1}\left(\frac{x^2-\lambda^2}{x}\right)^n dx\,y\,dy-n\beta\int_{y=\lambda_2}^{R_1}\int_{x=y}^{R_1}\left(\frac{x^2-\lambda^2}{x}\right)^{n-1}dx\,y\,dy\right.$$
$$\left.-\left(\frac{\lambda^2-\lambda_2^2}{2}\right)\left[\int_k^{\lambda_1}\left(\frac{\lambda^2-x^2}{x}\right)^n dx-n\beta\int_k^{\lambda_1}\left(\frac{\lambda^2-x^2}{x}\right)^{n-1}dx\right]\right\}$$
$$-2n\lambda P^n\log r\frac{d\lambda}{dt}\left\{\int_{y=\lambda_2}^{R_1}\int_{x=y}^{R_1}\left(\frac{x^2-\lambda^2}{x}\right)^n\frac{dx}{\left(x^2-\lambda^2\right)}y\,dy-(n-1)\beta\int_{y=\lambda_2}^{R_1}\int_{x=y}^{R_1}\left(\frac{x^2-\lambda^2}{x}\right)^{n-1}\frac{dx}{\left(x^2-\lambda^2\right)}y\,dy\right.$$
$$\left.+\left(\frac{\lambda^2-\lambda_2^2}{2}\right)\left[\int_k^{\lambda_1}\left(\frac{\lambda^2-x^2}{x}\right)^n\frac{dx}{\left(\lambda^2-x^2\right)}-(n-1)\beta\int_k^{\lambda_1}\left(\frac{\lambda^2-x^2}{x}\right)^{n-1}\frac{dx}{\left(\lambda^2-x^2\right)}\right]\right\}$$
$$+\frac{\left(R_1^2-\lambda_2^2\right)}{4}\left(1-R_1^2+2\lambda^2\log R_1+4P\lambda\log R_1\right)\log r-D(t)\log r \tag{A3.1}$$

Using Eqs. (46) and (A1.13) in Eq. (32) and then integrating the resulting equation from k to r with the help of the boundary condition (39) and simplifying, we get the correction to velocity distribution u_{1H} in the region $k\le r\le\lambda_1$ as

$$u_{1H}^{+}=n^2P^{2n-2}\frac{dP}{dt}\left\{\int_{z=k}^{r}\int_{y=z}^{\lambda_1}\int_{x=k}^{y}\left(\frac{\lambda^2-x^2}{x}\right)^n dx\,y\,dy\,f_1(z,t)\,dz\right.$$
$$-n\beta\int_{z=k}^{r}\int_{y=z}^{\lambda_1}\int_{x=k}^{y}\left(\frac{\lambda^2-x^2}{x}\right)^{n-1}dx\,y\,dy\,f_1(z,t)\,dz$$
$$\left.+\left(\frac{\lambda^2-\lambda_1^2}{2}\right)\left[\int_{z=k}^{r}\int_{x=k}^{\lambda_1}\left(\frac{\lambda^2-x^2}{x}\right)^n dx\,f_1(z,t)\,dz-n\beta\int_{z=k}^{r}\int_{x=k}^{\lambda_1}\left(\frac{\lambda^2-x^2}{x}\right)^{n-1}dx\,f_1(z,t)\,dz\right]\right\}$$
$$+2n^2\lambda P^{2n-1}\frac{d\lambda}{dt}\left\{\int_{z=k}^{r}\int_{y=z}^{\lambda_1}\int_{x=k}^{y}\left(\frac{\lambda^2-x^2}{x}\right)^n\frac{dx}{\left(\lambda^2-x^2\right)}y\,dy\,f_1(z,t)\,dz\right.$$
$$-(n-1)\beta\int_{z=k}^{r}\int_{y=z}^{\lambda_1}\int_{x=k}^{y}\left(\frac{\lambda^2-x^2}{x}\right)^{n-1}\frac{dx}{\left(\lambda^2-x^2\right)}y\,dy\,f_1(z,t)\,dz$$
$$\left.+\left(\frac{\lambda^2-\lambda_1^2}{2}\right)\left[\int_{z=k}^{r}\int_{x=k}^{\lambda_1}\left(\frac{\lambda^2-x^2}{x}\right)^n\frac{dx}{\left(\lambda^2-x^2\right)}f_1(z,t)\,dz-(n-1)\beta\int_{z=k}^{r}\int_{x=k}^{\lambda_1}\left(\frac{\lambda^2-x^2}{x}\right)^{n-1}\frac{dx}{\left(\lambda^2-x^2\right)}f_1(z,t)\,dz\right]\right\}$$
$$+nP^{n-1}D(t)\int_k^r f_1(z,t)\,dz \tag{A3.2}$$

where

$$f_1(z,t)=\frac{1}{z}\left[\left(\frac{\lambda^2-z^2}{z}\right)^{n-1}-(n-1)\beta\left(\frac{\lambda^2-z^2}{z}\right)^{n-2}\right] \tag{A3.3}$$

Using the condition $u_{1H}^{+}\big|_{r=\lambda_1}=u_{1p}$, the correction to plug flow velocity u_{1p} in the region $\lambda_1\le r\le\lambda_2$ is obtained from Eq. (A3.2) as

$$u_{1p}=n^2P^{2n-2}\frac{dP}{dt}\left\{\int_{z=k}^{\lambda_1}\int_{y=z}^{\lambda_1}\int_{x=k}^{y}\left(\frac{\lambda^2-x^2}{x}\right)^n dx\,y\,dy\,f_1(z,t)\,dz\right.$$
$$-n\beta\int_{z=k}^{\lambda_1}\int_{y=z}^{\lambda_1}\int_{x=k}^{y}\left(\frac{\lambda^2-x^2}{x}\right)^{n-1}dx\,y\,dy\,f_1(z,t)\,dz$$
$$\left.+\left(\frac{\lambda^2-\lambda_1^2}{2}\right)\left[\int_{z=k}^{\lambda_1}\int_{x=k}^{\lambda_1}\left(\frac{\lambda^2-x^2}{x}\right)^n dx\,f_1(z,t)\,dz-n\beta\int_{z=k}^{\lambda_1}\int_{x=k}^{\lambda_1}\left(\frac{\lambda^2-x^2}{x}\right)^{n-1}dx\,f_1(z,t)\,dz\right]\right\}$$
$$+2n^2\lambda P^{2n-1}\frac{d\lambda}{dt}\left\{\int_{z=k}^{\lambda_1}\int_{y=z}^{\lambda_1}\int_{x=k}^{y}\left(\frac{\lambda^2-x^2}{x}\right)^n\frac{dx}{\left(\lambda^2-x^2\right)}y\,dy\,f_1(z,t)\,dz\right.$$
$$-(n-1)\beta\int_{z=k}^{\lambda_1}\int_{y=z}^{\lambda_1}\int_{x=k}^{y}\left(\frac{\lambda^2-x^2}{x}\right)^{n-1}\frac{dx}{\left(\lambda^2-x^2\right)}y\,dy\,f_1(z,t)\,dz$$
$$\left.+\left(\frac{\lambda^2-\lambda_1^2}{2}\right)\left[\int_{z=k}^{\lambda_1}\int_{x=k}^{\lambda_1}\left(\frac{\lambda^2-x^2}{x}\right)^n\frac{dx}{\left(\lambda^2-x^2\right)}f_1(z,t)\,dz-(n-1)\beta\int_{z=k}^{\lambda_1}\int_{x=k}^{\lambda_1}\left(\frac{\lambda^2-x^2}{x}\right)^{n-1}\frac{dx}{\left(\lambda^2-x^2\right)}f_1(z,t)\,dz\right]\right\}$$
$$+nP^{n-1}D(t)\int_k^{\lambda_1} f_1(z,t)\,dz \tag{A3.4}$$

Substituting Eqs. (46) and (A1.15) in Eq. (36) and then integrating the resulting equation between r and R_1 with the help of the boundary condition (40) and Eq. (A3.1) and simplifying, we get the correction to velocity distribution u_{1H} in the region $\lambda_2 \le r \le R_1$ as

$$
\begin{aligned}
u_{1H}^{++} = & -\frac{1}{8}\frac{dP}{dt}\Big\{\left(1-R_1^2\right)+2R_1^2\log R_1-\frac{1}{3}\left(1-R_1^3\right)-R_1^4\log R_1 \\
& +\lambda^2\left[-4R_1^2\log R_1-2\left(1-R_1^2\right)+4\left(R_1\log R_1\right)^2\right]\Big\} \\
& -\frac{\lambda P}{2}\frac{d\lambda}{dt}\left[-R_1^2\log R_1-\frac{1}{2}\left(1-R_1^2\right)+2\left(R_1\log R_1\right)^2 -\frac{1}{3}\left(1-R_1^3\right)-R_1^4\log R_1\right] \\
& +nP^{n-1}\log R_1\frac{dP}{dt}\Big\{\int_{y=\lambda_2}^{R_1}\int_{x=y}^{R_1}\left(\frac{x^2-\lambda^2}{x}\right)^n dx\,y\,dy-n\beta \int_{y=\lambda_2}^{R_1}\int_{x=y}^{R_1}\left(\frac{x^2-\lambda^2}{x}\right)^{n-1} dx\,y\,dy \\
& -\left(\frac{\lambda^2-\lambda_2^2}{2}\right)\left[\int_k^{\lambda_1}\left(\frac{\lambda^2-x^2}{x}\right)^n dx-n\beta\int_k^{\lambda_1}\left(\frac{\lambda^2-x^2}{x}\right)^{n-1}dx\right]\Big\} \\
& -2n\lambda P^n\log R_1\frac{d\lambda}{dt} \Big\{\int_{y=\lambda_2}^{R_1}\int_{x=y}^{R_1}\left(\frac{x^2-\lambda^2}{x}\right)^n\frac{dx}{\left(x^2-\lambda^2\right)}y\,dy-(n-1)\beta \int_{y=\lambda_2}^{R_1}\int_{x=y}^{R_1}\left(\frac{x^2-\lambda^2}{x}\right)^{n-1}\frac{dx}{\left(x^2-\lambda^2\right)}y\,dy \\
& -\left(\frac{\lambda^2-\lambda_2^2}{2}\right)\left[\int_k^{\lambda_1}\left(\frac{\lambda^2-x^2}{x}\right)^n\frac{dx}{\left(\lambda^2-x^2\right)}-(n-1)\beta \int_k^{\lambda_1}\left(\frac{\lambda^2-x^2}{x}\right)^{n-1}\frac{dx}{\left(\lambda^2-x^2\right)}\right]\Big\} \\
& +\frac{\left(R_1^2-\lambda_2^2\right)}{4}\log R_1\left(1-R_1^2+2\lambda^2\log R_1 +4P\lambda\log R_1\right)-D(t)\log R_1 \\
& -n^2P^{2n-2}\frac{dP}{dt}\Big[\int_{z=r}^{R_1}\int_{y=\lambda_2}^{z}\int_{x=y}^{R_1}\left(\frac{x^2-\lambda^2}{x}\right)^n dx\,y\,dy\,f_2(z,t)\,dz-n\beta \int_{z=r}^{R_1}\int_{y=\lambda_2}^{z}\int_{x=y}^{R_1}\left(\frac{x^2-\lambda^2}{x}\right)^{n-1} dx\,y\,dy\,f_2(z,t)\,dz \\
& -\left(\frac{\lambda^2-\lambda_2^2}{2}\right)\left[\int_{z=r}^{R_1}\int_{x=k}^{\lambda_1}\left(\frac{\lambda^2-x^2}{x}\right)^n dx\,f_2(z,t)\,dz-n\beta \int_{z=r}^{R_1}\int_{x=k}^{\lambda_1}\left(\frac{\lambda^2-x^2}{x}\right)^{n-1} dx\,f_2(z,t)\,dz\right]\Big\} \\
& +2n^2\lambda P^{2n-1}\frac{d\lambda}{dt}\Big\{\int_{z=r}^{R_1}\int_{y=\lambda_2}^{z}\int_{x=y}^{R_1}\left(\frac{x^2-\lambda^2}{x}\right)^n \frac{dx}{\left(x^2-\lambda^2\right)}y\,dy\,f_2(z,t)\,dz \\
& -(n-1)\beta\int_{z=r}^{R_1}\int_{y=\lambda_2}^{z}\int_{x=y}^{R_1}\left(\frac{x^2-\lambda^2}{x}\right)^{n-1}\frac{dx}{\left(x^2-\lambda^2\right)}y\,dy\,f_2(z,t)\,dz \\
& +\left(\frac{\lambda^2-\lambda_2^2}{2}\right)\Big[\int_{z=r}^{R_1}\int_{x=k}^{\lambda_1}\left(\frac{\lambda^2-x^2}{x}\right)^n\frac{dx}{\left(\lambda^2-x^2\right)}f_2(z,t)\,dz \\
& -(n-1)\beta\int_{z=r}^{R_1}\int_{x=k}^{\lambda_1}\left(\frac{\lambda^2-x^2}{x}\right)^{n-1}\frac{dx}{\left(\lambda^2-x^2\right)}f_2(z,t)\,dz\Big]\Big\} \\
& -\frac{nP^{n-1}}{4}\left(1-R_1^2+2\lambda^2\log R_1+4\lambda P\log R_1\right) \\
& \int_r^{R_1}\left(z^2-\lambda_2^2\right)f_2(z,t)\,dz+nP^{n-1}D(t)\int_r^{R_1}f_2(z,t)\,dz
\end{aligned}
\tag{A3.4}
$$

where

$$
f_2(z,t)=\frac{1}{z}\left[\left(\frac{z^2-\lambda^2}{z}\right)^{n-1}-(n-1)\beta\left(\frac{z^2-\lambda^2}{z}\right)^{n-2}\right] \tag{A3.5}
$$

The continuity of the velocity distribution gives

$$
u_{1H}^{+}(\lambda_1,t)=u_{1p}=u_{1H}^{++}(\lambda_2,t) \tag{A3.6}
$$

The expression for $D(t)$ is obtained by using Eqs. (A3.2) and (A3.5) in Eq. (A3.6) and is given below

$$
\begin{aligned}
D(t)= & \frac{n^2P^{2n-2}}{\left(I_2-I_1-E\right)}\frac{dP}{dt} \Big\{\int_{z=k}^{\lambda_1}\int_{y=z}^{\lambda_1}\int_{x=k}^{y}\left(\frac{\lambda^2-x^2}{x}\right)^n dx\,y\,dy\,f_1(z,t)\,dz \\
& -n\beta\int_{z=k}^{\lambda_1}\int_{y=z}^{\lambda_1}\int_{x=k}^{y}\left(\frac{\lambda^2-x^2}{x}\right)^{n-1} dx\,y\,dy\,f_1(z,t)\,dz \\
& +\left(\frac{\lambda^2-\lambda_1^2}{2}\right)\left[\int_{z=k}^{\lambda_1}\int_{x=k}^{\lambda_1}\left(\frac{\lambda^2-x^2}{x}\right)^n dx\,f_1(z,t)\,dz-n\beta \int_{z=k}^{\lambda_1}\int_{x=k}^{\lambda_1}\left(\frac{\lambda^2-x^2}{x}\right)^{n-1} dx\,f_1(z,t)\,dz\right]\Big\} \\
& +\frac{2n^2\lambda P^{2n-1}}{\left(I_2-I_1-E\right)}\frac{d\lambda}{dt}
\end{aligned}
$$

$$\left\{\int_{z=k}^{\lambda_1}\int_{y=z}^{\lambda_1}\int_{x=k}^{y}\left(\frac{\lambda^2-x^2}{x}\right)^n\frac{dx}{\left(\lambda^2-x^2\right)}\,y\,dy\,f_1(z,t)\,dz\right.$$

$$-(n-1)\beta\int_{z=k}^{\lambda_1}\int_{y=z}^{\lambda_1}\int_{x=k}^{y}\left(\frac{\lambda^2-x^2}{x}\right)^{n-1}\frac{dx}{\left(\lambda^2-x^2\right)}\,y\,dy\,f_1(z,t)\,dz$$

$$+\left(\frac{\lambda^2-\lambda_1^2}{2}\right)\left[\int_{z=k}^{\lambda_1}\int_{x=k}^{\lambda_1}\left(\frac{\lambda^2-x^2}{x}\right)^n\frac{dx}{\left(\lambda^2-x^2\right)}f_1(z,t)\,dz\right.$$

$$\left.\left.-(n-1)\beta\int_{z=k}^{\lambda_1}\int_{x=k}^{\lambda_1}\left(\frac{\lambda^2-x^2}{x}\right)^{n-1}\frac{dx}{\left(\lambda^2-x^2\right)}f_1(z,t)\,dz\right]\right\}$$

$$+\frac{1}{8\left(I_2-I_1-E\right)}\frac{dP}{dt}$$

$$\left\{\left(1-R_1^2\right)+2R_1^2\log R_1-\frac{1}{3}\left(1-R_1^3\right)-R_1^4\log R_1\right.$$

$$\left.+\lambda^2\left[-4R_1^2\log R_1-2\left(1-R_1^2\right)+4\left(R_1\log R_1\right)^2\right]\right\}$$

$$+\frac{\lambda P}{2\left(I_2-I_1-E\right)}\frac{d\lambda}{dt}$$

$$\left[-R_1^2\log R_1-\frac{1}{2}\left(1-R_1^2\right)+2\left(R_1\log R_1\right)^2-\frac{1}{3}\left(1-R_1^3\right)-R_1^4\log R_1\right]$$

$$-\frac{nP^{n-1}\log R_1}{\left(I_2-I_1-E\right)}\frac{dP}{dt}$$

$$\left\{\int_{y=\lambda_2}^{R_1}\int_{x=y}^{R_1}\left(\frac{x^2-\lambda^2}{x}\right)^n dx\,y\,dy-n\beta\int_{y=\lambda_2}^{R_1}\int_{x=y}^{R_1}\left(\frac{x^2-\lambda^2}{x}\right)^{n-1}dx\,y\,dy\right.$$

$$\left.-\left(\frac{\lambda^2-\lambda_2^2}{2}\right)\left[\int_k^{\lambda_1}\left(\frac{\lambda^2-x^2}{x}\right)^n dx-n\beta\int_k^{\lambda_1}\left(\frac{\lambda^2-x^2}{x}\right)^{n-1}dx\right]\right\}$$

$$+\frac{2n\lambda P^n\log R_1}{\left(I_2-I_1-E\right)}\frac{d\lambda}{dt}\left\{\int_{y=\lambda_2}^{R_1}\int_{x=y}^{R_1}\left(\frac{x^2-\lambda^2}{x}\right)^n\frac{dx}{\left(x^2-\lambda^2\right)}\,y\,dy\right.$$

$$-(n-1)\beta\int_{y=\lambda_2}^{R_1}\int_{x=y}^{R_1}\left(\frac{x^2-\lambda^2}{x}\right)^{n-1}\frac{dx}{\left(x^2-\lambda^2\right)}\,y\,dy$$

$$+\left(\frac{\lambda^2-\lambda_2^2}{2}\right)\left[\int_k^{\lambda_1}\left(\frac{\lambda^2-x^2}{x}\right)^n\frac{dx}{\left(\lambda^2-x^2\right)}-(n-1)\beta\right.$$

$$\left.\left.\int_k^{\lambda_1}\left(\frac{\lambda^2-x^2}{x}\right)^{n-1}\frac{dx}{\left(\lambda^2-x^2\right)}\right\}\right]$$

$$-\frac{\left(R_1^2-\lambda_2^2\right)}{4\left(I_2-I_1-E\right)}\log R_1$$

$$\left(1-R_1^2+2\lambda^2\log R_1+4P\lambda\log R_1\right)$$

$$+\frac{n^2P^{2n-2}}{\left(I_2-I_1-E\right)}\frac{dP}{dt}$$

$$\left\{\int_{z=\lambda_2}^{R_1}\int_{y=\lambda_2}^{z}\int_{x=y}^{R_1}\left(\frac{x^2-\lambda^2}{x}\right)^n dx\,y\,dy\,f_2(z,t)\,dz\right.$$

$$-n\beta\int_{z=\lambda_2}^{R_1}\int_{y=\lambda_2}^{z}\int_{x=y}^{R_1}\left(\frac{x^2-\lambda^2}{x}\right)^{n-1}dx\,y\,dy\,f_2(z,t)\,dz$$

$$-\left(\frac{\lambda^2-\lambda_2^2}{2}\right)\left[\int_{z=\lambda_2}^{R_1}\int_{x=k}^{\lambda_1}\left(\frac{\lambda^2-x^2}{x}\right)^n dx\,f_2(z,t)\,dz-n\beta\right.$$

$$\left.\left.\int_{z=\lambda_2}^{R_1}\int_{x=k}^{\lambda_1}\left(\frac{\lambda^2-x^2}{x}\right)^{n-1}dx\,f_2(z,t)\,dz\right]\right\}$$

$$-\frac{2n^2\lambda P^{2n-1}}{\left(I_2-I_1-E\right)}\frac{d\lambda}{dt}$$

$$\left\{\int_{z=\lambda_2}^{R_1}\int_{y=\lambda_2}^{z}\int_{x=y}^{R_1}\left(\frac{x^2-\lambda^2}{x}\right)^n\frac{dx}{\left(x^2-\lambda^2\right)}\,y\,dy\,f_2(z,t)\,dz\right.$$

$$-(n-1)\beta\int_{z=\lambda_2}^{R_1}\int_{y=\lambda_2}^{z}\int_{x=y}^{R_1}\left(\frac{x^2-\lambda^2}{x}\right)^{n-1}$$

$$\frac{dx}{\left(x^2-\lambda^2\right)}\,y\,dy\,f_2(z,t)\,dz$$

$$+\left(\frac{\lambda^2-\lambda_2^2}{2}\right)\left[\int_{z=\lambda_2}^{R_1}\int_{x=k}^{\lambda_1}\left(\frac{\lambda^2-x^2}{x}\right)^n\frac{dx}{\left(\lambda^2-x^2\right)}f_2(z,t)\,dz\right.$$

$$\left.\left.-(n-1)\beta\int_{z=\lambda_2}^{R_1}\int_{x=k}^{\lambda_1}\left(\frac{\lambda^2-x^2}{x}\right)^{n-1}\frac{dx}{\left(\lambda^2-x^2\right)}f_2(z,t)\,dz\right]\right\}$$

$$+\frac{nP^{n-1}}{4\left(I_2-I_1-E\right)}\left(1-R_1^2+2\lambda^2\log R_1+4\lambda P\log R_1\right)$$

$$\int_{\lambda_2}^{R_1}\left(z^2-\lambda_2^2\right)f_2(z,t)\,dz \tag{A3.7}$$

where

$$I_2-I_1-E=nP^{n-1}$$

$$\left(\int_{\lambda_2}^{R_1}f_2(z,t)\,dz-\int_k^{\lambda_1}f_1(z,t)\,dz\right)-\log R_1 \tag{A3.8}$$

Appendix 4

The volumetric flow rate as in Eq. (47), we have

$$Q=8\int_k^1 ru\,dr$$

$$=8\left(\int_k^{\lambda_1}u_H^+\,r\,dr+\int_{\lambda_1}^{\lambda_2}u_p\,r\,dr+\int_{\lambda_2}^{R_1}u_H^{++}\,r\,dr+\int_{R_1}^{1}u_N\,r\,dr\right)$$

$$=8\left[\left(\int_k^{\lambda_1}u_{0H}^+\,r\,dr+\int_{\lambda_1}^{\lambda_2}u_{0p}\,r\,dr+\int_{\lambda_2}^{R_1}u_{0H}^{++}\,r\,dr+\int_{R_1}^{1}u_{0N}\,r\,dr\right)\right.$$

$$+\alpha_H^2\left(\int_k^{\lambda_1} u_{1H}^{+}\, r\,dr+\int_{\lambda_1}^{\lambda_2} u_{1p}\, r\,dr+\int_{\lambda_2}^{R_1} u_{1H}^{++}\, r\,dr\right)+\alpha_N^2\int_{R_1}^{1} u_{1N}\, r\,dr\Bigg]$$
$$=8\left(Q_1+Q_2+Q_3+Q_4\right)+8\alpha_H^2\left(Q_5+Q_6+Q_7\right)+8\alpha_N^2 Q_8 \qquad \text{(A4.1)}$$

Substituting Eq. (50) in $Q_1 \otimes$ of Eq. (A4.1), we get

$$Q_1=P^n\left[\int_{r=k}^{\lambda_1}\int_{x=k}^{r}\left(\frac{\lambda^2-x^2}{x}\right)^n dx\, r\,dr-n\beta \int_{r=k}^{\lambda_1}\int_{x=k}^{r}\left(\frac{\lambda^2-x^2}{x}\right)^{n-1} dx\, r\,dr\right] \qquad \text{(A4.2)}$$

Change of order of integrals in Eq. (A4.2) gives

$$Q_1=P^n\left[\int_k^{\lambda_1}\left(\frac{\lambda_1^2-x^2}{2}\right)\left(\frac{\lambda^2-x^2}{x}\right)^n dx-n\beta \int_k^{\lambda_1}\left(\frac{\lambda_1^2-x^2}{2}\right)\left(\frac{\lambda^2-x^2}{x}\right)^{n-1} dx\right] \qquad \text{(A4.3)}$$

Using Eq. (51) in Q_2 of Eq. (A4.1), one can get

$$Q_2=P^n\left[\int_k^{\lambda_1}\left(\frac{\lambda_2^2-\lambda_1^2}{2}\right)\left(\frac{\lambda^2-x^2}{x}\right)^n dx-n\beta \int_k^{\lambda_1}\left(\frac{\lambda_2^2-\lambda_1^2}{2}\right)\left(\frac{\lambda^2-x^2}{x}\right)^{n-1} dx\right] \qquad \text{(A4.4)}$$

Substitution of Eq. (52) in Q_3 of Eq. (A4.1) yields

$$Q_3=P^n\left[\int_{r=\lambda_2}^{R_1}\int_{x=r}^{R_1}\left(\frac{x^2-\lambda^2}{x}\right)^n dx\, rdr- n\beta\int_{r=\lambda_2}^{R_1}\int_{x=r}^{R_1}\left(\frac{x^2-\lambda^2}{x}\right)^{n-1} dx\, rdr\right] +\frac{P}{4}\left(R_1^2-\lambda_2^2\right)\left(1-R_1^2+2\lambda^2\log R_1\right) \qquad \text{(A4.5)}$$

Change of order of integrals in (A4.5) gives

$$Q_3=P^n\left[\int_{\lambda_2}^{R_1}\left(\frac{x^2-\lambda_2^2}{2}\right)\left(\frac{x^2-\lambda^2}{x}\right)^n dx- n\beta\int_{\lambda_2}^{R_1}\left(\frac{x^2-\lambda_2^2}{2}\right)\left(\frac{x^2-\lambda^2}{x}\right)^{n-1} dx\right] +\frac{P}{4}\left(R_1^2-\lambda_2^2\right)\left(1-R_1^2+2\lambda^2\log R_1\right) \qquad \text{(A4.6)}$$

Using Eq. (49) in Q_4 of Eq. (A4.1) gives

$$Q_4=\frac{P}{8}\left[1-R_1^2-4\lambda^2\left(1-R_1^2\right)\log R_1\right] \qquad \text{(A4.7)}$$

Substituting Eqs. (A4.3), (A4.4), (A4.6) and (A4.7) in the first part of Eq. (A4.1) and then simplifying, one can obtain

$$\begin{aligned}&8\left(Q_1+Q_2+Q_3+Q_4\right)\\&=4P^n\Bigg\{-\int_k^{\lambda_1}\left(\frac{\lambda^2-x^2}{x}\right)^n x^2dx+n\beta\int_k^{\lambda_1}\left(\frac{\lambda^2-x^2}{x}\right)^{n-1} x^2dx\\&+\int_{\lambda_2}^{R_1}\left(\frac{x^2-\lambda^2}{x}\right)^n x^2dx-n\beta\int_{\lambda_2}^{R_1}\left(\frac{x^2-\lambda^2}{x}\right)^{n-1} x^2dx\\&+\lambda_2^2\left[\int_k^{\lambda_1}\left(\frac{\lambda^2-x^2}{x}\right)^n dx-n\beta\int_k^{\lambda_1}\left(\frac{\lambda^2-x^2}{x}\right)^{n-1} dx\right]\\&-\lambda_2^2\left[\int_{\lambda_2}^{R_1}\left(\frac{x^2-\lambda^2}{x}\right)^n dx-n\beta\int_{\lambda_2}^{R_1}\left(\frac{x^2-\lambda^2}{x}\right)^{n-1} dx\right]\Bigg\}\\&+P\left[2\left(R_1^2-\lambda_2^2\right)\left(1-R_1^2+2\lambda^2\log R_1\right)\right.\\&\left.+1-R_1^2-4\lambda^2\left(1-R_1^2\right)\log R_1\right]\end{aligned} \qquad \text{(A4.8)}$$

The condition (54) gives

$$P^n\left\{\int_k^{\lambda_1}\left(\frac{\lambda^2-r^2}{r}\right)^n dr-\int_{\lambda_2}^{R_1}\left(\frac{r^2-\lambda^2}{r}\right)^n dr- n\beta\left[\int_k^{\lambda_1}\left(\frac{\lambda^2-r^2}{r}\right)^{n-1} dr-\int_{\lambda_2}^{R_1}\left(\frac{r^2-\lambda^2}{r}\right)^{n-1} dr\right]\right\} =\frac{P}{2}\left[1-R_1^2+2\lambda^2\log\left(R_1\right)\right] \qquad \text{(A4.9)}$$

Using Eq. (A4.9) in Eq. (A4.8), we get

$$\begin{aligned}&8\left(Q_1+Q_2+Q_3+Q_4\right)\\&=4P^n\Bigg\{-\int_k^{\lambda_1}\left(\frac{\lambda^2-x^2}{x}\right)^n x^2dx+\int_{\lambda_2}^{R_1}\left(\frac{x^2-\lambda^2}{x}\right)^n x^2dx\\&+n\beta\left[\int_k^{\lambda_1}\left(\frac{\lambda^2-x^2}{x}\right)^{n-1} x^2dx-\int_{\lambda_2}^{R_1}\left(\frac{x^2-\lambda^2}{x}\right)^{n-1} x^2dx\right]\Bigg\}\\&+P\left[1-R_1^2+2\left(1-R_1^4\right)-2\lambda_2^2\left(1-R_1^2\right)\right.\\&\left.+4\lambda^2\left(2R_1^2-\lambda_2^2\right)\log R_1\right]\end{aligned} \qquad \text{(A4.10)}$$

Using Eq. (A3.2) in Q_5 of Eq. (A4.1), we obtain

$$Q_5=n^2P^{2n-2}\frac{dP}{dt}\left\{\int_{r=k}^{\lambda_1}\int_{z=k}^{r}\int_{y=z}^{\lambda_1}\int_{x=k}^{y}\left(\frac{\lambda^2-x^2}{x}\right)^n dx\, y\,dy\, f_1\left(z,t\right)dz\, r\,dr\right.$$

$$-n\beta \int_{r=k}^{\lambda_1} \int_{z=k}^{r} \int_{y=z}^{\lambda_1} \int_{x=k}^{y} \left(\frac{\lambda^2 - x^2}{x}\right)^{n-1} dx\, y\, dy\, f_1(z,t)\, dz\, r\, dr$$

$$+\left(\frac{\lambda^2 - \lambda_1^2}{2}\right)\left[\int_{r=k}^{\lambda_1} \int_{z=k}^{r} \int_{x=k}^{\lambda_1} \left(\frac{\lambda^2 - x^2}{x}\right)^{n} dx\, f_1(z,t)\, dz\, r\, dr\right.$$

$$\left.\left. -n\beta \int_{r=k}^{\lambda_1} \int_{z=k}^{r} \int_{x=k}^{\lambda_1} \left(\frac{\lambda^2 - x^2}{x}\right)^{n} dx\, f_1(z,t)\, dz\, r\, dr\right]\right\}$$

$$+2n^2 \lambda P^{2n-1} \frac{d\lambda}{dt}$$

$$\left\{\int_{r=k}^{\lambda_1} \int_{z=k}^{r} \int_{y=z}^{\lambda_1} \int_{x=k}^{y} \left(\frac{\lambda^2 - x^2}{x}\right)^{n} \frac{dx}{(\lambda^2 - x^2)}\, y\, dy\, f_1(z,t)\, dz\, r\, dr\right.$$

$$-(n-1)\beta$$

$$\int_{r=k}^{\lambda_1} \int_{z=k}^{r} \int_{y=z}^{\lambda_1} \int_{x=k}^{y} \left(\frac{\lambda^2 - x^2}{x}\right)^{n-1} \frac{dx}{(\lambda^2 - x^2)}\, y\, dy\, f_1(z,t)\, dz\, r\, dr$$

$$+\left[\left(\frac{\lambda^2 - \lambda_1^2}{2}\right)\int_{r=k}^{\lambda_1} \int_{z=k}^{r} \int_{x=k}^{\lambda_1} \left(\frac{\lambda^2 - x^2}{x}\right)^{n} \frac{dx}{(\lambda^2 - x^2)} f_1(z,t)\, dz\, r\, dr\right.$$

$$\left.\left. -(n-1)\beta \int_{r=k}^{\lambda_1} \int_{z=k}^{r} \int_{x=k}^{\lambda_1} \left(\frac{\lambda^2 - x^2}{x}\right)^{n-1} \frac{dx}{(\lambda^2 - x^2)} f_1(z,t)\, dz\, r\, dr\right]\right\}$$

$$+nP^{n-1} D(t) \int_{r=k}^{\lambda_1} \int_{z=k}^{r} f_1(z,t)\, dz\, r\, dr \qquad \text{(A4.11)}$$

Using Eq. (A3.4) in Q_6 of Eq. (A4.1), we have

$$Q_6 = \left(\frac{\lambda_2^2 - \lambda_1^2}{2}\right) u_{1p} = \left(\frac{\lambda_2^2 - \lambda_1^2}{2}\right) n^2 P^{2n-2}$$

$$\frac{dP}{dt}\left\{\int_{z=k}^{\lambda_1} \int_{y=z}^{\lambda_1} \int_{x=k}^{y} \left(\frac{\lambda^2 - x^2}{x}\right)^{n} dx\, y\, dy\, f_1(z,t)\, dz\right.$$

$$-n\beta \int_{z=k}^{\lambda_1} \int_{y=z}^{\lambda_1} \int_{x=k}^{y} \left(\frac{\lambda^2 - x^2}{x}\right)^{n-1} dx\, y\, dy\, f_1(z,t)\, dz$$

$$+\left(\frac{\lambda^2 - \lambda_1^2}{2}\right)\left[\int_{z=k}^{\lambda_1} \int_{x=k}^{\lambda_1} \left(\frac{\lambda^2 - x^2}{x}\right)^{n} dx\, f_1(z,t)\, dz\right.$$

$$\left.\left. -n\beta \int_{z=k}^{\lambda_1} \int_{x=k}^{\lambda_1} \left(\frac{\lambda^2 - x^2}{x}\right)^{n-1} dx\, f_1(z,t)\, dz\right]\right\}$$

$$+\left(\frac{\lambda_2^2 - \lambda_1^2}{2}\right) 2n^2 P^{2n-1} \frac{d\lambda}{dt}$$

$$\left\{\int_{z=k}^{\lambda_1} \int_{y=z}^{\lambda_1} \int_{x=k}^{y} \left(\frac{\lambda^2 - x^2}{x}\right)^{n} \frac{dx}{(\lambda^2 - x^2)}\, y\, dy\, f_1(z,t)\, dz\right.$$

$$-(n-1)\beta \int_{z=k}^{\lambda_1} \int_{y=z}^{\lambda_1} \int_{x=k}^{y} \left(\frac{\lambda^2 - x^2}{x}\right)^{n-1} \frac{dx}{(\lambda^2 - x^2)}\, y\, dy\, f_1(z,t)\, dz$$

$$+\left(\frac{\lambda^2 - \lambda_1^2}{2}\right)\left[\int_{z=k}^{\lambda_1} \int_{x=k}^{\lambda_1} \left(\frac{\lambda^2 - x^2}{x}\right)^{n} \frac{dx}{(\lambda^2 - x^2)} f_1(z,t)\, dz\right.$$

$$\left.\left. -(n-1))\beta \int_{z=k}^{\lambda_1} \int_{x=k}^{\lambda_1} \left(\frac{\lambda^2 - x^2}{x}\right)^{n-1} \frac{dx}{(\lambda^2 - x^2)} f_1(z,t)\, dz\right]\right\}$$

$$+\left(\frac{\lambda_2^2 - \lambda_1^2}{2}\right) nP^{n-1} D(t) \int_{k}^{\lambda_1} f_1(z,t)\, dz$$

$$\text{(A4.12)}$$

Use of Eq. (A3.4) in Q_7 of Eq. (A4.1) yields

$$Q_7 = -\left(\frac{R_1^2 - \lambda_2^2}{16}\right)\frac{dP}{dt}$$

$$\left[\left(1 - R_1^2\right) + 2R_1^2 \log R_1 - \frac{1}{3}\left(1 - R_1^3\right) - R_1^4 \log R_1\right.$$

$$\left. +\lambda^2\left\{-4R_1^2 \log R_1 - 2\left(1 - R_1^2\right) + 4\left(R_1 \log R_1\right)^2\right\}\right]$$

$$-\left(\frac{R_1^2 - \lambda_2^2}{4}\right)\lambda P \frac{d\lambda}{dt}\left[-R_1^2 \log R_1 - \frac{1}{2}\left(1 - R_1\right) + \right.$$

$$\left. 2\left(R_1 \log R_1\right)^2 - \frac{1}{3}\left(1 - R_1^3\right) - R_1^4 \log R_1\right]$$

$$+\left(\frac{R_1^2 - \lambda_2^2}{2}\right) nP^{n-1} \log R_1 \frac{dP}{dt}$$

$$\left\{\int_{y=\lambda_2}^{R_1} \int_{x=y}^{R_1} \left(\frac{x^2 - \lambda^2}{x}\right)^{n} dx\, y\, dy - n\beta \int_{y=\lambda_2}^{R_1} \int_{x=y}^{R_1} \left(\frac{x^2 - \lambda^2}{x}\right)^{n-1} dx\, y\, dy\right.$$

$$\left. -\left(\frac{\lambda^2 - \lambda_2^2}{2}\right)\left[\int_{k}^{\lambda_1} \left(\frac{\lambda^2 - x^2}{x}\right)^{n} dx - n\beta \int_{k}^{\lambda_1} \left(\frac{\lambda^2 - x^2}{x}\right)^{n-1} dx\right]\right\}$$

$$-\left(\frac{R_1^2 - \lambda_2^2}{2}\right) 2n\lambda P^n \log R_1 \frac{d\lambda}{dt}\left\{\int_{y=\lambda_2}^{R_1} \int_{x=y}^{R_1} \left(\frac{x^2 - \lambda^2}{x}\right)^{n} \frac{dx}{(x^2 - \lambda^2)}\, y\, dy\right.$$

$$-(n-1)\beta \int_{y=\lambda_2}^{R_1} \int_{x=y}^{R_1} \left(\frac{x^2 - \lambda^2}{x}\right)^{n-1} \frac{dx}{(x^2 - \lambda^2)}\, y\, dy$$

$$+\left(\frac{\lambda^2 - \lambda_2^2}{2}\right)\left[\int_{k}^{\lambda_1} \left(\frac{\lambda^2 - x^2}{x}\right)^{n} \frac{dx}{(\lambda^2 - x^2)} - \right.$$

$$\left.\left. (n-1)\beta \int_{k}^{\lambda_1} \left(\frac{\lambda^2 - x^2}{x}\right)^{n-1} \frac{dx}{(\lambda^2 - x^2)}\right]\right\}$$

$$+\frac{\left(R_1^2 - \lambda_2^2\right)^2 \log R_1}{8}\left[1 - R_1^2 + 2\lambda^2 \log R_1 + 4P\lambda \log R_1\right]$$

$$-n^2 P^{2n-2} \frac{dP}{dt}\left\{\int_{r=\lambda_2}^{R_1} \int_{z=r}^{R_1} \int_{y=\lambda_2}^{z} \int_{x=y}^{R_1} \left(\frac{x^2 - \lambda^2}{x}\right)^{n} dx\, y\, dy\, f_2(z,t)\, dz\, r\, dr\right.$$

$$-n\beta \int_{r=\lambda_2}^{R_1} \int_{z=r}^{R_1} \int_{y=\lambda_2}^{z} \int_{x=y}^{R_1} \left(\frac{x^2 - \lambda^2}{x}\right)^{n-1} dx\, y\, dy\, f_2(z,t)\, dz\, r\, dr$$

$$-\left(\frac{\lambda^2-\lambda_2^2}{2}\right)\left[\int_{r=\lambda_2}^{R_1}\int_{z=r}^{R_1}\int_{x=k}^{\lambda_1}\left(\frac{\lambda^2-x^2}{x}\right)^n dx\, f_2(z,t)\,dz\,r\,dr\right.$$

$$\left.-n\beta\int_{r=\lambda_2}^{R_1}\int_{z=r}^{R_1}\int_{x=k}^{\lambda_1}\left(\frac{\lambda^2-x^2}{x}\right)^{n-1} dx\, f_2(z,t)\,dz\,r\,dr\right]\Bigg\}$$

$$+2n^2\lambda P^{2n-1}\frac{d\lambda}{dt}\Bigg\{\int_{r=\lambda_2}^{R_1}\int_{z=r}^{R_1}\int_{y=\lambda_2}^{z}\int_{x=y}^{R_1}\left(\frac{x^2-\lambda^2}{x}\right)^n \frac{dx}{\left(x^2-\lambda^2\right)}\,y\,dy\, f_2(z,t)\,dz\,r\,dr$$

$$-(n-1)\beta\int_{r=\lambda_2}^{R_1}\int_{z=r}^{R_1}\int_{y=\lambda_2}^{z}\int_{x=y}^{R_1}\left(\frac{x^2-\lambda^2}{x}\right)^{n-1} \frac{dx}{\left(x^2-\lambda^2\right)}\,y\,dy\, f_2(z,t)\,dz\,r\,dr$$

$$+\left(\frac{\lambda^2-\lambda_2^2}{2}\right)\left[\int_{r=\lambda_2}^{R_1}\int_{z=r}^{R_1}\int_{x=k}^{\lambda_1}\left(\frac{\lambda^2-x^2}{x}\right)^n \frac{dx}{\left(x^2-\lambda^2\right)} f_2(z,t)\,dz\,r\,dr\right.$$

$$\left.-(n-1)\beta\int_{r=\lambda_2}^{R_1}\int_{z=r}^{R_1}\int_{x=k}^{\lambda_1}\left(\frac{\lambda^2-x^2}{x}\right)^{n-1} \frac{dx}{\left(\lambda^2-x^2\right)} f_2(z,t)\,dz\,r\,dr\right]\Bigg\}$$

$$-\frac{nP^{n-1}}{4}\left(1-R_1^2+2\lambda^2\log R_1+4P\lambda\log R_1\right)\int_{r=\lambda_2}^{R_1}\int_{z=r}^{R_1}\left(z^2-\lambda_2^2\right)f_2(z,t)\,dz\,r\,dr$$

$$+D(t)\left[-\left(\frac{R_1^2-\lambda_2^2}{2}\right)\log R_1+nP^{n-1}\int_{r=\lambda_2}^{R_1}\int_{z=r}^{R_1}f_2(z,t)\,dz\,r\,dr\right] \quad \text{(A4.13)}$$

Using Eq. (A3.1) in Q8 of (A4.1), we get

$$Q_8=-\frac{1}{8}\frac{dP}{dt}\Bigg\{\frac{1}{3}\left(1-R_1^2\right)-\frac{1}{4}\left(1-R_1^4\right)-R_1^4\log R_1$$

$$+\frac{R_1^2}{2}\left(1-R_1^2\right)+\frac{1}{15}\left(1-R_1^5\right)+\frac{R_1^6}{2}\log R_1+\frac{R_1^4}{4}\left(1-R_1^2\right)$$

$$+\lambda^2\left[\frac{3R_1^4}{2}\log R_1+\frac{5}{8}\left(1-R_1^4\right)-\left(1-R_1^2\right)-2\left(R_1^2\log R_1\right)^2\right.$$

$$\left.-R_1^2\left(1-R_1^2\right)\log R_1+\frac{R_1^2}{2}\left(1-R_1^2\right)\right]\Bigg\}$$

$$-\frac{\lambda P}{2}\frac{d\lambda}{dt}\left[\frac{1}{16}\left(1-R_1^4\right)+\frac{R_1^4}{4}\log R_1-\right.$$

$$\frac{5}{12}\left(1-R_1^2\right)+\frac{1}{8}\left(1-R_1^4\right)-\left(R_1^2\log R_1\right)^2$$

$$\left.-\frac{R_1^2}{2}\left(1-R_1^2\right)\log R_1+\frac{1}{15}\left(1-R_1^5\right)+\frac{R_1^6}{2}\log R_1+\frac{R_1^4}{4}\left(1-R_1^2\right)\right]$$

$$-nP^{n-1}\left[\frac{R_1^2}{2}\log R_1+\frac{1}{4}\left(1-R_1^2\right)\right]\frac{dP}{dt}$$

$$\Bigg\{\int_{y=\lambda_2}^{R_1}\int_{x=y}^{R_1}\left(\frac{x^2-\lambda^2}{x}\right)^n dx\,y\,dy-n\beta\int_{y=\lambda_2}^{R_1}\int_{x=y}^{R_1}\left(\frac{x^2-\lambda^2}{x}\right)^{n-1}dx\,y\,dy$$

$$-\left(\frac{\lambda^2-\lambda_2^2}{2}\right)\left[\int_{k}^{\lambda_1}\left(\frac{\lambda^2-x^2}{x}\right)^n dx-n\beta\int_{k}^{\lambda_1}\left(\frac{\lambda^2-x^2}{x}\right)^{n-1}dx\right]\Bigg\}$$

$$+2n\lambda P^n\left[\frac{R_1^2}{2}\log R_1+\frac{1}{4}\left(1-R_1^2\right)\right]\frac{d\lambda}{dt}$$

$$\Bigg\{\int_{y=\lambda_2}^{R_1}\int_{x=y}^{R_1}\left(\frac{x^2-\lambda^2}{x}\right)^n \frac{dx}{\left(x^2-\lambda^2\right)}\,y\,dy$$

$$-(n-1)\beta\int_{y=\lambda_2}^{R_1}\int_{x=y}^{R_1}\left(\frac{x^2-\lambda^2}{x}\right)^{n-1}\frac{dx}{\left(x^2-\lambda^2\right)}\,y\,dy$$

$$+\left(\frac{\lambda^2-\lambda_2^2}{2}\right)\left[\int_{k}^{\lambda_1}\left(\frac{\lambda^2-x^2}{x}\right)^n\frac{dx}{\left(\lambda^2-x^2\right)}-\right.$$

$$\left.(n-1)\beta\int_{k}^{\lambda_1}\left(\frac{\lambda^2-x^2}{x}\right)^{n-1}\frac{dx}{\left(\lambda^2-x^2\right)}\right]\Bigg\}$$

$$-\left(\frac{R_1^2-\lambda_2^2}{2}\right)\left[\frac{R_1^2}{2}\log R_1+\frac{1}{4}\left(1-R_1^2\right)\right]$$

$$\left(1-R_1^2+2\lambda^2\log R_1+4P\lambda\log R_1\right)$$

$$+D(t)\left[\frac{R_1^2}{2}\log R_1+\frac{1}{4}\left(1-R_1^2\right)\right] \quad \text{(A4.14)}$$

Substitution of Eqs. (A4.10)-(A4.14) in Eq. (A4.1) yields the final expression for flow rate.

Dr. D. S. Sankar received his B. Sc degree in Mathematics from the University of Madras, India, in 1989. He then received his M .Sc, M. Phil and Ph.D. degrees from Anna University, India in 1991, 1992 and 2004, respectively. Dr. D. S. Sankar is currently working at the School of Mathematical Sciences, University Science Malaysia, Malaysia. He serves as a referee for several reputed international journals. Dr. D. S. Sankar's research interests include Fluid Dynamics, Hemodynamics, Differential Equations and Numerical Analysis.

Dr. Usik Lee received his B.S. degree in Mechanical Engineering from Yonsei University, Korea in 1979. He then received his M.S. and Ph.D. degrees in Mechanical Engineering from Stanford University, USA in 1982 and 1985, respectively. Dr. Lee is currently a Professor at the Department of Mechanical Engineering at Inha University in Incheon, Korea. He serves as a referee for many reputed international journals. Dr. Lee's research interests include structural dynamics, biomechanics, and computational mechanics.